
DIFUSCO: Graph-based Diffusion Solvers for Combinatorial Optimization

Zhiqing Sun¹ Yiming Yang¹

Abstract

Neural network-based Combinatorial Optimization (CO) methods have shown promising results in solving various NP-complete (NPC) problems without relying on hand-crafted domain knowledge. This paper broadens the current scope of neural solvers for NPC problems by introducing a new graph-based diffusion framework, namely DIFUSCO. Our framework casts NPC problems as discrete $\{0, 1\}$ -vector optimization problems and leverages graph-based denoising diffusion models to generate high-quality solutions. We investigate two types of diffusion models with Gaussian and Bernoulli noise, respectively, and devise an effective inference schedule to enhance the solution quality. We evaluate our methods on two well-studied NPC combinatorial optimization problems: Traveling Salesman Problem (TSP) and Maximal Independent Set (MIS). Experimental results show that DIFUSCO strongly outperforms the previous state-of-the-art neural solvers, improving the performance gap between ground-truth and neural solvers from 1.76% to **0.46%** on TSP-500, from 2.46% to **1.17%** on TSP-1000, and from 3.19% to **2.58%** on TSP-10000. For the MIS problem, DIFUSCO outperforms the previous state-of-the-art neural solver on the challenging SATLIB benchmark. Our code is available at <https://github.com/Edward-Sun/DIFUSCO>.

icant expert efforts to approximate near-optimal solutions (Arora, 1996; Gonzalez, 2007).

Recent development in deep learning has shown new promise in solving NPC problems. Existing neural CO solvers for NPC problems can be roughly classified into three categories based on how the solutions are generated, i.e., the autoregressive constructive solvers, the non-autoregressive constructive solvers, and the improvement heuristics solvers. Methods in the first category use autoregressive factorization to sequentially grow a valid partial solution (Bello et al., 2016; Kool et al., 2019a). Those methods typically suffer from the costly computation in their sequential decoding parts and hence are difficult to scale up to large problems (Fu et al., 2021). Methods in the second category rely on non-autoregressive modeling for scaling up, with a conditional independence assumption among variables as typical (Joshi et al., 2019; Karalias & Loukas, 2020; Qiu et al., 2022). Such an assumption, however, unavoidably limits the capability of those methods to capture the multimodal nature of the problems (Khalil et al., 2017; Gu et al., 2018). Methods in the third category (improvement heuristics solvers) use a Markov decision process (MDP) to iteratively refines an existing feasible solution with neural network-guided local operations such as 2-opt (Lin & Kernighan, 1973; Andrade et al., 2012) and node swap (Chen & Tian, 2019; Wu et al., 2021). These methods have also suffered from the difficulty in scaling up and the latency in inference, partly due to the sparse rewards and sample efficiency issues when learning improvement heuristics in a reinforcement learning (RL) framework (Wu et al., 2021; Ma et al., 2021).

1. Introduction

Combinatorial Optimization (CO) problems are mathematical problems that involve finding the optimal solution in a discrete space. They are fundamental challenges in computer science, especially the NP-Complete (NPC) class of problems, which are believed to be intractable in polynomial time. Traditionally, NPC solvers rely on integer programming (IP) or hand-crafted heuristics, which demand signif-

Motivated by the recent remarkable success of diffusion models in probabilistic generation (Song & Ermon, 2019; Ho et al., 2020; Rombach et al., 2022; Yu et al.; Saharia et al., 2022b), we introduce a novel approach named DIFUSCO, which stands for the graph-based DIFfusion Solvers for Combinatorial Optimization. To apply the iterative denoising process of diffusion models to graph-based settings, we formulate each NPC problem as a $\{0, 1\}$ -valued vector with N variables that indicate the selection of nodes or edges in the candidate solutions for the task. Then we use a message passing-based graph neural network (Kipf & Welling, 2016; Hamilton et al., 2017; Gilmer et al., 2017; Veličković et al., 2018) to encode each instance graph and to denoise the

¹Carnegie Mellon University, Pittsburgh, PA 15213, USA. Correspondence to: Zhiqing Sun <zhiqing@cs.cmu.edu>.

corrupted variables. Such a graph-based diffusion model overcomes the limitations of previous neural NPC solvers from a new perspective. Firstly, DIFUSCO can perform inference on all variables in parallel with a few ($\ll N$) denoising steps (Sec. 3.3), avoiding the sequential generation problem of autoregressive constructive solvers. Secondly, DIFUSCO can model a multimodal distribution via iterative refinements, which alleviates the expressiveness limitation of previous non-autoregressive constructive models. Last but not least, DIFUSCO is trained in an efficient and stable manner with supervised denoising (Sec. 3.2), which solves the training scalability issue of RL-based improvement heuristics methods.

We should point out that the idea of utilizing a diffusion-based generative model for NPC problems has been explored recently in the literature. In particular, Graikos et al. (2022) proposed an image-based diffusion model to solve Euclidean Traveling Salesman problems by projecting each TSP instance onto a 64×64 greyscale image space and then using a Convolutional Neural Network (CNN) to generate the predicted solution image. The main difference between such *image-based* diffusion solver and our *graph-based* diffusion solver is that the latter can explicitly model the node/edge selection process via the corresponding random variables, which is a natural design choice for formulating NPC problems (since most of them are defined over a graph), while the former does not support such a desirable formalism. Although graph-based modeling has been employed with both constructive (Kool et al., 2019a) and improvement heuristics (d O Costa et al., 2020) solvers, how to use graph-based diffusion models for solving NPC problems has not been studied before, to the best of our knowledge.

We investigate two types of probabilistic diffusion within the DIFUSCO framework: continuous diffusion with Gaussian noise (Chen et al., 2022) and discrete diffusion with Bernoulli noise (Austin et al., 2021; Hoogeboom et al., 2021). These two types of diffusion models have been applied to image processing but not to NPC problems. We systematically compare the two types of modeling and find that discrete diffusion performs better than continuous diffusion by a significant margin (Section 4). We also design an effective inference strategy to enhance the generation quality of the discrete diffusion solvers.

Finally, we demonstrate that a single graph neural network architecture, namely the Anisotropic Graph Neural Network (Bresson & Laurent, 2018; Joshi et al., 2022), can be used as the backbone network for two different NP-complete combinatorial optimization problems: Traveling Salesman Problem (TSP) and Maximal Independent Set (MIS). Our experimental results show that DIFUSCO outperforms previous probabilistic NPC solvers on benchmark datasets of TSP and MIS problems with various sizes.

2. Related Work

Let us outline the related work in several categories below. Additional related work can be found in Appendix A.

2.1. Autoregressive Construction Heuristics Solvers

Autoregressive models have achieved state-of-the-art results as constructive heuristic solvers for combinatorial optimization (CO) problems, following their recent success in the language modeling or text generation domain (Vaswani et al., 2017; Brown et al., 2020). The approach, first proposed by Bello et al. (2016) for CO problems, uses a neural network and reinforcement learning to append one new variable to the partial solution at each decoding step until a complete solution is generated. However, autoregressive models (Kool et al., 2019a) face high time and space complexity challenges for large-scale NPC problems due to their sequential generation scheme and quadratic complexity in the self-attention mechanism (Vaswani et al., 2017).

2.2. Non-autoregressive Construction Heuristics Solvers

Non-autoregressive (or heatmap) constructive heuristics solvers (Joshi et al., 2019; Fu et al., 2021; Geisler et al., 2022; Qiu et al., 2022) are recently proposed to address this scalability issue by assuming conditional independence among variables in NPC problems, but this assumption limits the ability to capture the multimodal nature (Khalil et al., 2017; Gu et al., 2018) of high-quality solution distributions. Therefore, additional active search (Bello et al., 2016; Qiu et al., 2022) or Monte-Carlo Tree Search (MCTS) (Fu et al., 2021; Silver et al., 2016) are needed to further improve the expressive power of the non-autoregressive scheme.

DIFUSCO can be regarded as a member in the non-autoregressive constructive heuristics category and thus can be benefited from heatmap search techniques such as MCTS. But DIFUSCO uses an iterative denoising scheme to generate the final heatmap, which significantly enhances its expressive power compared to previous non-autoregressive methods.

2.3. Diffusion Models for Discrete Data

Typical diffusion models (Sohl-Dickstein et al., 2015; Song & Ermon, 2019; Ho et al., 2020; Song & Ermon, 2020; Nichol & Dhariwal, 2021; Karras et al., 2022) operate in the continuous domain, progressively adding Gaussian noise to the clean data in the forward process, and learning to remove noises in the reverse process in a discrete-time framework.

Discrete diffusion models have been proposed for the generation of discrete image bits or texts using binomial noises (Sohl-Dickstein et al., 2015) and multinomial/categorical

noises (Austin et al., 2021; Hoogeboom et al., 2021). Recent research has also shown the potential of discrete diffusion models in sound generation (Yang et al., 2022), protein structure generation (Luo et al., 2022), molecule generation (Vignac et al., 2022), and better text generation (Johnson et al., 2021; He et al., 2022).

Another line of work studies diffusion models for discrete data by applying continuous diffusion models with Gaussian noise on the embedding space of discrete data (Gong et al., 2022; Li et al., 2022; Dieleman et al., 2022), the $\{-1.0, 1.0\}$ real-number vector space (Chen et al., 2022), and the simplex space (Han et al., 2022). The most relevant work might be Niu et al. (2020), which proposed a continuous score-based generative framework for graphs, but they only evaluated simple non-NP-hard CO tasks such as Shortest Path and Maximum Spanning Tree.

3. DIFUSCO: Proposed Approach

3.1. Problem Definition

Following a conventional notation (Papadimitriou & Steiglitz, 1998), we define $\mathcal{X}_s = \{0, 1\}^N$ as the space of discrete solutions $\{\mathbf{x}\}$ for a CO problem instance s , and $c_s : \mathcal{X}_s \rightarrow \mathbb{R}$ as the objective function for solutions $\mathbf{x} \in \mathcal{X}_s$:

$$c_s(\mathbf{x}) = \text{cost}(\mathbf{x}, s) + \text{valid}(\mathbf{x}, s) \quad (1)$$

where $\text{cost}(\cdot)$ is the cost function for a feasible solution and is simply a linear function of \mathbf{x} in most NP-complete problems; $\text{valid}(\cdot)$ is the validation function that returns 0 for feasible solutions and $+\infty$ for invalid solutions. The optimization objective is to find the optimal solution for a given instance s :

$$\mathbf{x}^{s*} = \underset{\mathbf{x} \in \mathcal{X}_s}{\text{argmin}} c_s(\mathbf{x}). \quad (2)$$

This framework is generically applicable to different NPC problems. For example, for the Traveling Salesman Problem (TSP), $\mathbf{x} \in \{0, 1\}^N$ is the indicator vector for selecting a subset from N edges; the cost of this subset is calculated as: $\text{cost}_{\text{TSP}}(\mathbf{x}, s) = \sum_i x_i \cdot d_i^{(s)}$, where $d_i^{(s)}$ denotes the weight of the i -th edge in problem instance s , and the $\text{valid}(\cdot)$ part of Formula (1) ensures that \mathbf{x} is a tour that visits each node exactly once and returns to the starting node at the end. For the Maximal Independent Set (MIS) problem, $\mathbf{x} \in \{0, 1\}^N$ is the indicator vector for selecting a subset from N nodes; the cost of the subset is calculated as: $\text{cost}_{\text{MIS}}(\mathbf{x}, s) = \sum_i (1 - x_i)$, and the corresponding $\text{valid}(\cdot)$ validates \mathbf{x} is an independent set where each node in the set has no connection to any other node in the set.

Probabilistic neural NPC solvers (Bello et al., 2016) tackle instance problem s by defining a parameterized conditional distribution $p_\theta(\mathbf{x}|s)$, such that the expected cost

$\sum_{\mathbf{x} \in \mathcal{X}_s} c_s(\mathbf{x}) \cdot p(\mathbf{x}|s)$ is minimized. Such probabilistic generative models are usually optimized by reinforcement learning algorithms (Williams, 1992; Konda & Tsitsiklis, 2000). In this paper, assuming the optimal (or high-quality) solution \mathbf{x}_s^* is available for each training instance s , we optimize the model through supervised learning. Let $\mathcal{S} = \{s_i\}_1^N$ be independent and identically distributed (IID) training samples for a type of NPC problem, we aim to maximize the likelihood of optimal (or high-quality) solutions, where the loss function L is defined as:

$$L(\theta) = \mathbb{E}_{s \in \mathcal{S}} [-\log p_\theta(\mathbf{x}_s^{s*}|s)] \quad (3)$$

Next, we describe how to use diffusion models to parameterize the generative distribution p_θ . For brevity, we omit the conditional notations of s and denote \mathbf{x}^{s*} as \mathbf{x}_0 as a convention in diffusion models for all formulas in the next two sub-sections.

3.2. Diffusion Models in DIFUSCO

From the variational inference perspective (Kingma et al., 2021), diffusion models (Sohl-Dickstein et al., 2015; Ho et al., 2020; Song & Ermon, 2019) are latent variable models of the form $p_\theta(\mathbf{x}_0) := \int p_\theta(\mathbf{x}_{0:T}) d\mathbf{x}_{1:T}$, where $\mathbf{x}_1, \dots, \mathbf{x}_T$ are latents of the same dimensionality as the data $\mathbf{x}_0 = q(\mathbf{x}_0)$. The joint distribution

$$p_\theta(\mathbf{x}_{0:T}) = p(\mathbf{x}_T) \prod_{t=1}^T p_\theta(\mathbf{x}_{t-1}|\mathbf{x}_t) \quad (4)$$

is the learned reverse (denoising) process that gradually denoises the latent variables toward the data distribution, while the forward process

$$q(\mathbf{x}_{1:T}|\mathbf{x}_0) = \prod_{t=1}^T q(\mathbf{x}_t|\mathbf{x}_{t-1}) \quad (5)$$

gradually corrupts the data into noised latent variables. Training is performed by optimizing the usual variational bound on negative log-likelihood:

$$\begin{aligned} \mathbb{E} [-\log p_\theta(\mathbf{x}_0)] &\leq \mathbb{E}_q \left[-\log \frac{p_\theta(\mathbf{x}_{0:T})}{q(\mathbf{x}_{1:T}|\mathbf{x}_0)} \right] \\ &= \mathbb{E}_q \left[\sum_{t>1} D_{KL}[q(\mathbf{x}_{t-1}|\mathbf{x}_t, \mathbf{x}_0) \| p_\theta(\mathbf{x}_{t-1}|\mathbf{x}_t)] \right. \\ &\quad \left. - \log p_\theta(\mathbf{x}_0|\mathbf{x}_1) \right] + C \end{aligned} \quad (6)$$

where C is a constant.

Discrete Diffusion In discrete diffusion models with multinomial noises (Austin et al., 2021; Hoogeboom et al., 2021), the forward process is defined as:

$$q(\mathbf{x}_t|\mathbf{x}_{t-1}) = \text{Cat}(\mathbf{x}_t; \mathbf{p} = \mathbf{x}_{t-1}\mathbf{Q}_t), \quad (7)$$

where $\mathbf{Q}_t = \begin{bmatrix} (1 - \beta_t) & \beta_t \\ \beta_t & (1 - \beta_t) \end{bmatrix}$ is the transition probability matrix. $\mathbf{x}\mathbf{Q}$ is a row vector-matrix product where \mathbf{x} is to be understood as one-hot vectors $\{0, 1\}^{N \times 2}$ converted from the original $\mathbf{x} \in \{0, 1\}^N$.

Here, β_t denotes the corruption ratio. Also, we want $\prod_{t=1}^T (1 - \beta_t) \approx 0$ such that $\mathbf{x}_T \sim \text{Uniform}(\cdot)$. The t -step marginal can thus be written as:

$$q(\mathbf{x}_t | \mathbf{x}_0) = \text{Cat}(\mathbf{x}_t; \mathbf{p} = \mathbf{x}_0 \overline{\mathbf{Q}}_t), \quad (8)$$

where $\overline{\mathbf{Q}}_t = \mathbf{Q}_1 \mathbf{Q}_2 \dots \mathbf{Q}_t$. And the posterior at time $t - 1$ can be obtained by Bayes' theorem:

$$\begin{aligned} q(\mathbf{x}_{t-1} | \mathbf{x}_t, \mathbf{x}_0) &= \frac{q(\mathbf{x}_t | \mathbf{x}_{t-1}, \mathbf{x}_0) q(\mathbf{x}_{t-1} | \mathbf{x}_0)}{q(\mathbf{x}_t | \mathbf{x}_0)} \\ &= \text{Cat}\left(\mathbf{x}_{t-1}; \mathbf{p} = \frac{\mathbf{x}_t \mathbf{Q}_t^\top \odot \mathbf{x}_0 \overline{\mathbf{Q}}_{t-1}}{\mathbf{x}_0 \overline{\mathbf{Q}}_t \mathbf{x}_t^\top}\right), \end{aligned} \quad (9)$$

where \odot denotes the element-wise multiplication.

According to Austin et al. (2021), the denoising neural network is trained to predict the clean data $p_\theta(\tilde{\mathbf{x}}_0 | \mathbf{x}_t)$, and the reverse process is obtained by substituting the predicted $\tilde{\mathbf{x}}_0$ as \mathbf{x}_0 in Eq. 9:

$$p_\theta(\mathbf{x}_{t-1} | \mathbf{x}_t) = \sum_{\tilde{\mathbf{x}}} q(\mathbf{x}_{t-1} | \mathbf{x}_t, \tilde{\mathbf{x}}_0) p_\theta(\tilde{\mathbf{x}}_0 | \mathbf{x}_t) \quad (10)$$

Continuous Diffusion for Discrete Data The continuous diffusion models (Song & Ermon, 2019; Ho et al., 2020) can also be directly applied to discrete data by lifting the discrete input into a continuous space (Chen et al., 2022). Since the continuous diffusion models usually start from a standard Gaussian distribution $\epsilon \sim \mathcal{N}(\mathbf{0}, \mathbf{I})$, Chen et al. (2022) proposed to first rescale the $\{0, 1\}$ -valued variables \mathbf{x}_0 to the $\{-1, 1\}$ domain as $\hat{\mathbf{x}}_0$, and then treat them as real values. The forward process in continuous diffusion is defined as:

$$q(\hat{\mathbf{x}}_t | \hat{\mathbf{x}}_{t-1}) := \mathcal{N}(\hat{\mathbf{x}}_t; \sqrt{1 - \beta_t} \hat{\mathbf{x}}_{t-1}, \beta_t \mathbf{I}) \quad (11)$$

Again, β_t denotes the corruption ratio, and we want $\prod_{t=1}^T (1 - \beta_t) \approx 0$ such that $\mathbf{x}_T \sim \mathcal{N}(\cdot)$. The t -step marginal can thus be written as:

$$q(\hat{\mathbf{x}}_t | \hat{\mathbf{x}}_0) := \mathcal{N}(\hat{\mathbf{x}}_t; \sqrt{\bar{\alpha}_t} \hat{\mathbf{x}}_0, (1 - \bar{\alpha}_t) \mathbf{I}) \quad (12)$$

where $\alpha_t = 1 - \beta_t$ and $\bar{\alpha}_t = \prod_{\tau=1}^t \alpha_\tau$. Similar to Eq. 9, the posterior at time $t - 1$ can be obtained by Bayes' theorem:

$$q(\hat{\mathbf{x}}_{t-1} | \hat{\mathbf{x}}_t, \mathbf{x}_0) = \frac{q(\hat{\mathbf{x}}_t | \hat{\mathbf{x}}_{t-1}, \hat{\mathbf{x}}_0) q(\hat{\mathbf{x}}_{t-1} | \hat{\mathbf{x}}_0)}{q(\hat{\mathbf{x}}_t | \hat{\mathbf{x}}_0)}, \quad (13)$$

which is a closed-form Gaussian distribution (Ho et al., 2020). In continuous diffusion, the denoising neural network is trained to predict the unscaled Gaussian noise

$\tilde{\epsilon}_t = (\hat{\mathbf{x}}_t - \sqrt{\bar{\alpha}_t} \hat{\mathbf{x}}_0) / \sqrt{1 - \bar{\alpha}_t} = f_\theta(\hat{\mathbf{x}}_t, t)$. The reverse process (Ho et al., 2020) can use a point estimation of $\hat{\mathbf{x}}_0$ in the posterior:

$$p_\theta(\hat{\mathbf{x}}_{t-1} | \hat{\mathbf{x}}_t) = q\left(\hat{\mathbf{x}}_{t-1} | \hat{\mathbf{x}}_t, \frac{\hat{\mathbf{x}}_t - \sqrt{1 - \bar{\alpha}_t} f_\theta(\hat{\mathbf{x}}_t, t)}{\sqrt{\bar{\alpha}_t}}\right) \quad (14)$$

For generating discrete data, after the continuous data $\hat{\mathbf{x}}_0$ is generated, a thresholding/quantization operation is applied to convert them back to $\{0, 1\}$ -valued variables \mathbf{x}_0 as the model's prediction.

3.3. Denoising Schedule for Fast Inference

One way to speed up the inference of denoising diffusion models is to reduce the number of steps in the reverse diffusion process, which also reduces the number of neural network evaluations. The denoising diffusion implicit models (DDIMs) (Song et al., 2021a) are a class of models that apply this strategy in the continuous domain, and a similar approach can be used for discrete diffusion models (Austin et al., 2021).

Formally, when the forward process is defined not on all the latent variables $\mathbf{x}_{1:T}$, but on a subset $\{\mathbf{x}_{\tau_1}, \dots, \mathbf{x}_{\tau_M}\}$, where τ is an increasing sub-sequence of $[1, \dots, T]$ with length M , $\mathbf{x}_{\tau_1} = 1$ and $\mathbf{x}_{\tau_M} = T$, the fast sampling algorithms directly models $q(\mathbf{x}_{\tau_i-1} | \mathbf{x}_{\tau_i}, \mathbf{x}_0)$. Due to the space limit, the detailed algorithms are described in Appendix F.

We consider two types of denoising scheduled for τ given the desired $\text{card}(\tau) < T$: *linear* and *cosine*. The former uses timesteps such that $\tau_i = \lfloor ci \rfloor$ for some c , and the latter uses timesteps such that $\tau_i = \lfloor \cos(\frac{(1-ci)\pi}{2}) \cdot T \rfloor$ for some c . The intuition for the cosine schedule is that diffusion models can achieve better generation quality when iterating more steps in the low-noise regime (Nichol & Dhariwal, 2021; Yu et al., 2022; Chang et al., 2022).

3.4. Graph-based Denoising Network

The denoising network takes as input a set of noisy variables \mathbf{x}_t and the problem instance s and predicts the clean data $\tilde{\mathbf{x}}_0$. To balance both scalability and performance considerations, we adopt an anisotropic graph neural network with edge gating mechanisms (Bresson & Laurent, 2018; Joshi et al., 2022) as the backbone network for both discrete and continuous diffusion models, and the variables in the network output can be the states of either nodes, as in the case of Maximum Independent Set (MIS) problems, or edges, as in the case of Traveling Salesman Problems (TSP). The detailed description of neural network architectures can be found in Appendix G.

For TSP, the initial edge embeddings are initialized as the corresponding values in \mathbf{x}_t , and the initial node embeddings are initialized as sinusoidal positional features of the nodes.

For MIS, the initial edge embeddings are initialized as zeros, and the initial node embeddings are initialized as the corresponding values in \mathbf{x}_t . A 2-neuron and 1-neuron classification/regression head is applied to the final embeddings of for edges (or nodes) for discrete and continuous diffusion models, respectively.

3.5. Decoding Strategies for Diffusion-based Solvers

After the training of the parameterized denoising network according to Eq. 6, the solutions are sampled from the diffusion models $p_\theta(\mathbf{x}_0|s)$ for final evaluation. However, probabilistic generative models such as DIFUSCO cannot guarantee that the sampled solutions are feasible according to the definition of CO problems. Therefore, specialized decoding strategies are designed for the two CO problems studied in this paper.

Heatmap Generation The diffusion models $p_\theta(\cdot|s)$ produce discrete variables \mathbf{x} as the final predictions by applying Bernoulli sampling (Eq. 10) for discrete diffusion or quantization for continuous diffusion. However, this process discards the comparative information that reflects the confidence of the predicted variables, which is crucial for resolving conflicts in the decoding process. To preserve this information, we adapt the diffusion models to generate heatmaps (Joshi et al., 2019; Qiu et al., 2022) by making the following appropriate modifications: 1) For discrete diffusion, the final score of $p_\theta(\mathbf{x}_0 = 1|s)$ is preserved as the heatmap scores; 2) For continuous diffusion, we remove the final quantization and use $0.5(\hat{\mathbf{x}}_0 + 1)$ as the heatmap scores. Note that different from previous heatmap approaches (Joshi et al., 2019; Qiu et al., 2022) that produce a single conditionally independent distribution for all variables, DIFUSCO can produce diverse multimodal output distribution by using different random seeds.

TSP Decoding Let $\{A_{ij}\}$ be the heatmap scores generated by DIFUSCO denoting the confidence of each edge. We evaluate two approaches as the decoding method following previous work (Graikos et al., 2022; Qiu et al., 2022): 1) Greedy decoding (Graikos et al., 2022), where all the edges are ranked by $(A_{ij} + A_{ji})/\|\mathbf{c}_i - \mathbf{c}_j\|$, and are inserted into the partial solution if there are no conflicts. 2-opt heuristics (Lin & Kernighan, 1973) are optionally applied. 2) Monte Carlo Tree Search (MCTS) (Fu et al., 2021), where k -opt transformation actions are sampled guided by the heatmap scores to improve the current solutions. Due to the space limit, a detailed description of two decoding strategies can be found in Appendix E.

MIS Decoding Let $\{a_i\}$ be the heatmap scores generated by DIFUSCO denoting the confidence of each node. A greedy decoding strategy is used for the MIS problem,

where the nodes are ranked by a_i and inserted into the partial solution if there are no conflicts. Recent research (Böther et al., 2022) pointed out that the graph reduction and 2-opt search (Andrade et al., 2012) can find near-optimal solutions even starting from a randomly generated solution, so we do not use any post-processing for the greedy-decoded solutions.

Solution Sampling A common practice for probabilistic CO solvers (Kool et al., 2019a) is to sample multiple solutions and report the best one. For DIFUSCO, we follow this practice by sampling multiple heatmaps from $p_\theta(\mathbf{x}_0|s)$ with different random seeds and then applying the greedy decoding algorithm described above to each heatmap.

4. Experiments with TSP

We use 2-D Euclidean TSP instances to test our models. We generate these instances by randomly sampling nodes from a uniform distribution over the unit square. We use TSP-50 (with 50 nodes) as the main benchmark to compare different model configurations. We also evaluate our method on larger TSP instances with 100, 500, 1000, and 10000 nodes to demonstrate its scalability and performance against other state-of-the-art methods.

4.1. Experimental Settings

Datasets We generate and label the training instances using the Concorde exact solver (Applegate et al., 2006) for TSP-50/100 and the LKH-3 heuristic solver (Helsgaun, 2017) for TSP-500/1000/10000. We use the same test instances as (Joshi et al., 2022; Kool et al., 2019a) for TSP-50/100 and (Fu et al., 2021) for TSP-500/1000/10000.

Graph Sparsification We use sparse graphs for large-scale TSP problems to reduce the computational complexity. We sparsify the graphs by limiting each node to have only k edges to its nearest neighbors based on the Euclidean distances. We set k to 50 for TSP-500 and 100 for TSP-1000/10000. This way, we avoid the quadratic growth of edges in dense graphs as the number of nodes increases.

Model Settings $T = 1000$ denoising steps are used for the training of DIFUSCO on all datasets. Following Ho et al. (2020); Graikos et al. (2022), we use a simple linear noise schedule for $\{\beta_t\}_{t=1}^T$, where $\beta_1 = 10^{-4}$ and $\beta_T = 0.02$. We follow Graikos et al. (2022) and use the Greedy decoding + 2-opt scheme (Sec. 3.5) as the default decoding scheme for experiments.

Evaluation Metrics In order to compare the performance of different models, we present three metrics: average tour length (Length), average relative performance drop (Drop),

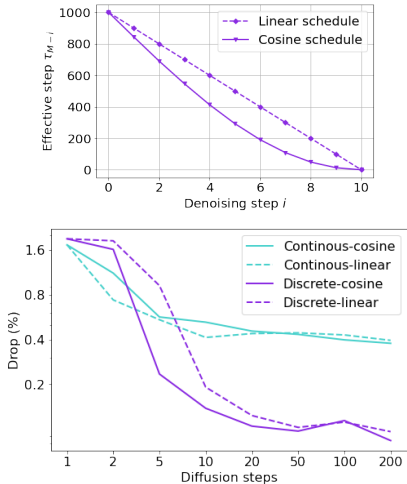


Figure 1: Comparison of continuous (Gaussian noise) and discrete (Bernoulli noise) diffusion models with different inference diffusion steps and inference schedule (linear v.s. cosine).

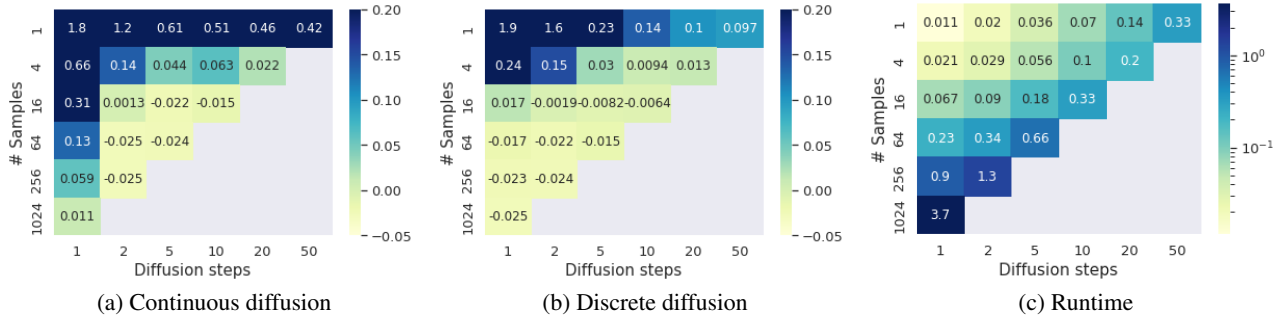


Figure 2: The performance Drop (%) are shown for continuous diffusion (a) and discrete diffusion (b) models on TSP-50 with different diffusion steps and number of samples. Their corresponding per-instance run-time (sec) are shown in (c), where the decomposed analysis (neural network + greedy decoding + 2-opt) can be found in the appendix (Tab. 5).

and total run time (Time). The detailed description can be found in Appendix D.

4.2. Design Analysis

Discrete Diffusion v.s. Continuous Diffusion We first investigate the suitability of two diffusion approaches for combinatorial optimization, namely continuous diffusion with Gaussian noise and discrete diffusion with Bernoulli noise (Sec. 3.2). Additionally, we explore the effectiveness of different denoising schedules, such as linear and cosine schedules (Sec. 3.3), on CO problems. To efficiently evaluate these model choices, we utilize the TSP-50 benchmark.

Note that although all the diffusion models are trained with a $T = 1000$ noise schedule, the inference schedule can be shorter than T , as described in Sec. 3.3. Specifically, we are interested in diffusion models with 1, 2, 5, 10, 20, 50, 100, and 200 diffusion steps.

Table 1: Comparing results on TSP-50 and TSP-100. * denotes the baseline for computing the performance drop. † indicates that the diffusion model samples a single solution as its greedy decoding scheme. Please refer to Sec. 4 for details.

ALGORITHM	TYPE	TSP-50		TSP-100	
		LENGTH↓	DROP(%)↓	LENGTH↓	DROP(%)↓
CONCORDE*	EXACT	5.69	0.00	7.76	0.00
2-OPT	HEURISTICS	5.86	2.95	8.03	3.54
AM	GREEDY	5.80	1.76	8.12	4.53
GCN	GREEDY	5.87	3.10	8.41	8.38
TRANSFORMER	GREEDY	5.71	0.31	7.88	1.42
POMO	GREEDY	5.73	0.64	7.84	1.07
SYM-NCO	GREEDY	-	-	7.84	0.94
DPDP	1k-IMPROVEMENTS	5.70	0.14	7.89	1.62
IMAGE DIFFUSION	GREEDY†	5.76	1.23	7.92	2.11
OURS	GREEDY†	5.70	0.10	7.78	0.24
AM	1k×SAMPLING	5.73	0.52	7.94	2.26
GCN	2k×SAMPLING	5.70	0.01	7.87	1.39
TRANSFORMER	2k×SAMPLING	5.69	0.00	7.76	0.39
POMO	8×AUGMENT	5.69	0.03	7.77	0.14
SYM-NCO	100×SAMPLING	-	-	7.79	0.39
MDAM	50×SAMPLING	5.70	0.03	7.79	0.38
DPDP	100k-IMPROVEMENTS	5.70	0.00	7.77	0.00
OURS	16×SAMPLING	5.69	-0.01	7.76	-0.01

Fig. 1 demonstrates the performance of two types of diffusion models with two types of inference schedules and various diffusion steps. We can see that discrete diffusion consistently outperforms the continuous diffusion models by a large margin when there are more than 5 diffusion steps¹. Besides, the cosine schedule is superior to linear on discrete diffusion and performs similarly on continuous diffusion. Therefore, we use cosine for the rest of the paper.

More Diffusion Iterations v.s. More Sampling By utilizing effective denoising schedules, diffusion models are able to adaptively infer based on the available computation budget by predetermining the total number of diffusion steps. This is similar to changing the number of samples in previous probabilistic neural NPC solvers (Kool et al., 2019a). Therefore, we investigate the trade-off between the number of diffusion iterations and the number of samples

¹We also observe similar patterns on TSP-100, where the results are reported in the appendix (Tab. 4).

Graph-based Diffusion Solvers for Combinatorial Optimization

Table 2: Results on large-scale TSP problems. RL, SL, AS, G, S, BS, and MCTS denotes Reinforcement Learning, Supervised Learning, Active Search, Greedy decoding, Sampling decoding, Beam-search, and Monte Carlo Tree Search, respectively. * indicates the baseline for computing the performance drop. Results of baselines are taken from Fu et al. (2021) and Qiu et al. (2022), so the runtime may not be directly comparable. See Section 4 and Appendix H for detailed descriptions.

ALGORITHM	TYPE	TSP-500			TSP-1000			TSP-10000		
		LENGTH ↓	DROP ↓	TIME ↓	LENGTH ↓	DROP ↓	TIME ↓	LENGTH ↓	DROP ↓	TIME ↓
CONCORDE	EXACT	16.55*	—	37.66m	23.12*	—	6.65h	N/A	N/A	N/A
GUROBI	EXACT	16.55	0.00%	45.63h	N/A	N/A	N/A	N/A	N/A	N/A
LKH-3 (DEFAULT)	HEURISTICS	16.55	0.00%	46.28m	23.12	0.00%	2.57h	71.77*	—	8.8h
LKH-3 (LESS TRAILS)	HEURISTICS	16.55	0.00%	3.03m	23.12	0.00%	7.73m	71.79	—	51.27m
FARTHEST INSERTION	HEURISTICS	18.30	10.57%	0s	25.72	11.25%	0s	80.59	12.29%	6s
AM	RL+G	20.02	20.99%	1.51m	31.15	34.75%	3.18m	141.68	97.39%	5.99m
GCN	SL+G	29.72	79.61%	6.67m	48.62	110.29%	28.52m	N/A	N/A	N/A
POMO+EAS-EMB	RL+AS+G	19.24	16.25%	12.80h	N/A	N/A	N/A	N/A	N/A	N/A
POMO+EAS-TAB	RL+AS+G	24.54	48.22%	11.61h	49.56	114.36%	63.45h	N/A	N/A	N/A
DIMES	RL+G	18.93	14.38%	0.97m	26.58	14.97%	2.08m	86.44	20.44%	4.65m
DIMES	RL+AS+G	17.81	7.61%	2.10h	24.91	7.74%	4.49h	80.45	12.09%	3.07h
OURS (DIFUSCO)	SL+G†	18.35	10.85%	3.61m	26.14	13.06%	11.86m	98.15	36.75%	28.51m
OURS (DIFUSCO)	SL+G†+2-OPT	16.80	1.49%	3.65m	23.56	1.90%	12.06m	73.99	3.10%	35.38m
EAN	RL+S+2-OPT	23.75	43.57%	57.76m	47.73	106.46%	5.39h	N/A	N/A	N/A
AM	RL+BS	19.53	18.03%	21.99m	29.90	29.23%	1.64h	129.40	80.28%	1.81h
GCN	SL+BS	30.37	83.55%	38.02m	51.26	121.73%	51.67m	N/A	N/A	N/A
DIMES	RL+S	18.84	13.84%	1.06m	26.36	14.01%	2.38m	85.75	19.48%	4.80m
DIMES	RL+AS+S	17.80	7.55%	2.11h	24.89	7.70%	4.53h	80.42	12.05%	3.12h
OURS (DIFUSCO)	SL+S	17.23	4.08%	11.02m	25.19	8.95%	46.08m	95.52	33.09%	6.59h
OURS (DIFUSCO)	SL+S+2-OPT	16.65	0.57%	11.46m	23.45	1.43%	48.09m	73.89	2.95%	6.72h
ATT-GCN	SL+MCTS	16.97	2.54%	2.20m	23.86	3.22%	4.10m	74.93	4.39%	21.49m
DIMES	RL+MCTS	16.87	1.93%	2.92m	23.73	2.64%	6.87m	74.63	3.98%	29.83m
DIMES	RL+AS+MCTS	16.84	1.76%	2.15h	23.69	2.46%	4.62h	74.06	3.19%	3.57h
OURS (DIFUSCO)	SL+MCTS	16.63	0.46%	10.13m	23.39	1.17%	24.47m	73.62	2.58%	47.36m

for diffusion-based NPC solvers.

Fig. 2 shows the results of continuous diffusion and discrete diffusion with various diffusion steps and number of parallel sampling, as well as their corresponding total run-time. The cosine denoising schedule is used for fast inference. Again, we find that discrete diffusion outperforms continuous diffusion across various settings. Besides, we find performing more diffusion iterations is generally more effective than sampling more solutions, even when the former uses less computation. For example, 20 (diffusion steps) \times 4 (samples) performs competitive to 1 (diffusion steps) \times 1024 (samples), while the runtime of the former is 18.5 \times less than the latter.

In general, we find that 50 (diffusion steps) \times 1 (samples) policy and 10 (diffusion steps) \times 16 (samples) policy make a good balance between exploration and exploitation for discrete DIFUSCO models and use them as the **Greedy** and **Sampling** strategies for the rest of the experiments.

4.3. Main Results

Comparison to SOTA Methods We compare discrete DIFUSCO to other state-of-the-art neural NPC solvers on TSP problems across various scales. Due to the space limit, the description of other baseline models can be found in

Appendix H.

Tab. 1 compare discrete DIFUSCO with other models on TSP-50 and TSP-100, where DIFUSCO achieves the state-of-the-art performance in both greedy and sampling settings for probabilistic solvers.

Tab. 2 compare discrete DIFUSCO with other models on the larger-scale TSP-500, TSP-1000, and TSP-10000 problems. Most previous probabilistic solvers (except DIMES (Qiu et al., 2022)) becomes untrainable on TSP problems of these scales, so the results of these models are reported with TSP-100 trained models. The results are reported with greedy, sampling, and MCTS decoding strategies, respectively. For fair comparisons (Fu et al., 2021; Qiu et al., 2022), MCTS decoding for TSP is always evaluated with only one sampled heatmap. From the table, we can see that DIFUSCO strongly outperforms the previous neural solvers on all three settings. In particular, with MCTS-based decoding, DIFUSCO significantly improving the performance gap between ground-truth and neural solvers from 1.76% to **0.46%** on TSP-500, from 2.46% to **1.17%** on TSP-1000, and from 3.19% to **2.58%** on TSP-10000.

Generalization Tests Finally, we study the generalization ability of discrete DIFUSCO trained on a set of TSP problems of a specific problem scale and evaluated on other prob-

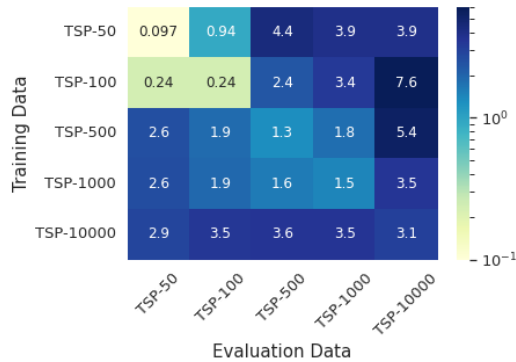


Figure 3: Generalization tests of DIFUSCO trained and evaluated on TSP problems across various scales. The performance Drop (%) with greedy decoding and 2-opt is reported.

lem scales. From Fig. 3, we can see that DIFUSCO has a strong generalization ability. In particular, the model trained with TSP-50 perform well on even TSP-1000 and TSP-10000. This pattern is different from the bad generalization ability of RL-trained or SL-trained non-autoregressive methods as reported in previous work (Joshi et al., 2022).

5. Experiments with MIS

For Maximal Independent Set (MIS), we experiment on two types of graphs that recent work (Li et al., 2018; Ahn et al., 2020; Böther et al., 2022; Qiu et al., 2022) shows struggles against, i.e., SATLIB (Hoos & Stützle, 2000) and Erdős-Rényi (ER) graphs (Erdős et al., 1960). The former is a set of graphs reduced from SAT instances in CNF, while the latter are random graphs. We use ER-[700-800] for evaluation, where ER-[n - N] indicates the graph contains n to N nodes. Following Qiu et al. (2022), the pairwise connection probability p is set to 0.15.

Datasets The training instances of labeled by the KaMIS² heuristic solver. The split of test instances on SAT datasets and the random-generated ER test graphs are taken from Qiu et al. (2022).

Model Settings The training schedule is the same as the TSP solver (Sec. 4.1). For SATLIB, we use discrete diffusion with 50 (diffusion steps) \times 1 (samples) policy and 50 (diffusion steps) \times 4 (samples) policy as the **Greedy** and **Sampling** strategies, respectively. For ER graphs, we use continuous diffusion with 50 (diffusion steps) \times 1 (samples) policy and 20 (diffusion steps) \times 8 (samples) policy as the **Greedy** and **Sampling** strategies, respectively.

²<https://github.com/KarlsruheMIS/KaMIS> (MIT License)

Table 3: Results on MIS problems. * indicates the baseline for computing the performance drop. RL, SL, G, S, and TS denotes Reinforcement Learning, Supervised Learning, Greedy decoding, Sampling decoding, and Tree Search, respectively. Please refer to Sec. 5 and Appendix H for details.

METHOD	TYPE	SATLIB			ER-[700-800]		
		SIZE \uparrow	DROP \downarrow	TIME \downarrow	SIZE \uparrow	DROP \downarrow	TIME \downarrow
KAMIS	HEURISTICS	425.96*	—	37.58m	44.87*	—	52.13m
GUROBI	EXACT	425.95	0.00%	26.00m	41.38	7.78%	50.00m
INTEL	SL+G	420.66	1.48%	23.05m	34.86	22.31%	6.06m
INTEL	SL+TS	N/A	N/A	N/A	38.80	13.43%	20.00m
DGL	SL+TS	N/A	N/A	N/A	37.26	16.96%	22.71m
LWD	RL+S	422.22	0.88%	18.83m	41.17	8.25%	6.33m
DIMES	RL+G	421.24	1.11%	24.17m	38.24	14.78%	6.12m
DIMES	RL+S	423.28	0.63%	20.26m	42.06	6.26%	12.01m
Ours	SL+G	424.50	0.34%	8.76m	38.83	12.40%	8.80m
Ours	SL+S	425.13	0.21%	23.74m	41.12	8.36%	26.67m

Evaluation Metrics We report the average size of the independent set (Size), average performance drop (Drop), and latency time (Time). The detailed description can be found in Appendix D. Notice that we disable graph reduction and 2-opt local search in all models for a fair comparison since it is pointed out by (Böther et al., 2022) that all models would perform similarly with local search post-processing.

Results and Analysis Tab. 3 compare discrete DIFUSCO with other baselines on SATLIB and ER-[700-800] benchmarks. We can see that DIFUSCO strongly outperforms previous state-of-the-art methods on SATLIB benchmark, reducing the gap between ground-truth and neural solvers from 0.63% to **0.21%**. However, we also found that DIFUSCO (especially with discrete diffusion in our preliminary experiments) does not perform well on the ER-[700-800] data. We hypothesize that this is because the previous methods usually use the node-based graph neural networks such as GCN (Kipf & Welling, 2017) or GraphSage (Hamilton et al., 2017) as the backbone network, while we use an edge-based Anisotropic GNN (Sec. 3.4), whose inductive bias may be not suitable for ER graphs.

6. Concluding Remarks

We proposed DIFUSCO, a novel graph-based diffusion model for solving NP-complete combinatorial optimization problems. We compared two variants of graph-based diffusion models: one with continuous Gaussian noise and one with discrete Bernoulli noise. We found that the discrete variant performs better than the continuous one. Moreover, we designed a cosine inference schedule that enhances the effectiveness of our model. DIFUSCO achieves state-of-the-art results on TSP and MIS problems, surpassing previous probabilistic NPC solvers in both accuracy and scalability.

For future work, we would like to explore the potential of

DIFUSCO in solving a broader range of NPC problems, including Mixed Integer Programming (Appendix C). We would also like to explore the use of equivariant graph neural networks (Xu et al., 2021; Hoogetboom et al., 2022) for further improvement of the diffusion models on geometrical NP-complete combinatorial optimization problems such as Euclidean TSP. Finally, we are interested in utilizing (higher-order) accelerated inference techniques for diffusion model-based solvers, such as those inspired by the continuous time framework for discrete diffusion (Campbell et al., 2022; Sun et al., 2022).

References

- Ahn, S., Seo, Y., and Shin, J. Learning what to defer for maximum independent sets. In *International Conference on Machine Learning*, pp. 134–144. PMLR, 2020.
- Andrade, D. V., Resende, M. G., and Werneck, R. F. Fast local search for the maximum independent set problem. *Journal of Heuristics*, 18(4):525–547, 2012.
- Applegate, D., Bixby, R., Chvatal, V., and Cook, W. Concorde TSP solver. <https://www.math.uwaterloo.ca/tsp/concorde/index.html>, 2006.
- Arora, S. Polynomial time approximation schemes for euclidean tsp and other geometric problems. In *Proceedings of 37th Conference on Foundations of Computer Science*, pp. 2–11. IEEE, 1996.
- Austin, J., Johnson, D. D., Ho, J., Tarlow, D., and van den Berg, R. Structured denoising diffusion models in discrete state-spaces. *Advances in Neural Information Processing Systems*, 34:17981–17993, 2021.
- Bello, I., Pham, H., Le, Q. V., Norouzi, M., and Bengio, S. Neural combinatorial optimization with reinforcement learning. *arXiv preprint arXiv:1611.09940*, 2016.
- Bi, J., Ma, Y., Wang, J., Cao, Z., Chen, J., Sun, Y., and Chee, Y. M. Learning generalizable models for vehicle routing problems via knowledge distillation. In *Advances in Neural Information Processing Systems*, 2022.
- Böther, M., Kißig, O., Taraz, M., Cohen, S., Seidel, K., and Friedrich, T. What’s wrong with deep learning in tree search for combinatorial optimization. In *International Conference on Learning Representations*, 2022. URL <https://openreview.net/forum?id=mk0HzdqY7il>.
- Bresson, X. and Laurent, T. An experimental study of neural networks for variable graphs. 2018.
- Bresson, X. and Laurent, T. The transformer network for the traveling salesman problem. *arXiv preprint arXiv:2103.03012*, 2021.
- Brown, T., Mann, B., Ryder, N., Subbiah, M., Kaplan, J. D., Dhariwal, P., Neelakantan, A., Shyam, P., Sastry, G., Askell, A., et al. Language models are few-shot learners. *Advances in neural information processing systems*, 33: 1877–1901, 2020.
- Campbell, A., Benton, J., Bortoli, V. D., Rainforth, T., Deligiannidis, G., and Doucet, A. A continuous time framework for discrete denoising models. In Oh, A. H., Agarwal, A., Belgrave, D., and Cho, K. (eds.), *Advances in Neural Information Processing Systems*, 2022. URL <https://openreview.net/forum?id=DmT862YAieY>.
- Chang, H., Zhang, H., Jiang, L., Liu, C., and Freeman, W. T. Maskgit: Masked generative image transformer. In *Proceedings of the IEEE/CVF Conference on Computer Vision and Pattern Recognition*, pp. 11315–11325, 2022.
- Chen, N., Zhang, Y., Zen, H., Weiss, R. J., Norouzi, M., and Chan, W. Wavegrad: Estimating gradients for waveform generation. In *International Conference on Learning Representations*, 2020.
- Chen, N., Zhang, Y., Zen, H., Weiss, R. J., Norouzi, M., Dehak, N., and Chan, W. Wavegrad 2: Iterative refinement for text-to-speech synthesis. *arXiv preprint arXiv:2106.09660*, 2021.
- Chen, T., Zhang, R., and Hinton, G. Analog bits: Generating discrete data using diffusion models with self-conditioning. *arXiv preprint arXiv:2208.04202*, 2022.
- Chen, X. and Tian, Y. Learning to perform local rewriting for combinatorial optimization. *Advances in Neural Information Processing Systems*, 32, 2019.
- Choo, J., Kwon, Y.-D., Kim, J., Jae, J., Hottung, A., Tierney, K., and Gwon, Y. Simulation-guided beam search for neural combinatorial optimization. In Oh, A. H., Agarwal, A., Belgrave, D., and Cho, K. (eds.), *Advances in Neural Information Processing Systems*, 2022. URL <https://openreview.net/forum?id=tYAS1Rpys5>.
- Croes, G. A. A method for solving traveling-salesman problems. *Operations research*, 6(6):791–812, 1958.
- d O Costa, P. R., Rhuggenaath, J., Zhang, Y., and Akcay, A. Learning 2-opt heuristics for the traveling salesman problem via deep reinforcement learning. In *Asian Conference on Machine Learning*, pp. 465–480. PMLR, 2020.
- da Costa, P. R. d. O., Rhuggenaath, J., Zhang, Y., and Akcay, A. Learning 2-OPT heuristics for the traveling salesman

- problem via deep reinforcement learning. *arXiv preprint arXiv:2004.01608*, 2020.
- Deudon, M., Cournut, P., Lacoste, A., Adulyasak, Y., and Rousseau, L.-M. Learning heuristics for the TSP by policy gradient. In *International conference on the integration of constraint programming, artificial intelligence, and operations research*, pp. 170–181. Springer, 2018.
- Dhariwal, P. and Nichol, A. Diffusion models beat gans on image synthesis. *Advances in Neural Information Processing Systems*, 34:8780–8794, 2021.
- Dieleman, S., Sartran, L., Roshannai, A., Savinov, N., Ganin, Y., Richemond, P. H., Doucet, A., Strudel, R., Dyer, C., Durkan, C., et al. Continuous diffusion for categorical data. *arXiv preprint arXiv:2211.15089*, 2022.
- Drori, I., Kharkar, A., Sickinger, W. R., Kates, B., Ma, Q., Ge, S., Dolev, E., Dietrich, B., Williamson, D. P., and Udell, M. Learning to solve combinatorial optimization problems on real-world graphs in linear time. In *2020 19th IEEE International Conference on Machine Learning and Applications (ICMLA)*, pp. 19–24. IEEE, 2020.
- Erdős, P., Rényi, A., et al. On the evolution of random graphs. *Publ. Math. Inst. Hung. Acad. Sci.*, 5(1):17–60, 1960.
- Fu, Z.-H., Qiu, K.-B., and Zha, H. Generalize a small pre-trained model to arbitrarily large tsp instances. In *Proceedings of the AAAI Conference on Artificial Intelligence*, volume 35, pp. 7474–7482, 2021.
- Geisler, S., Sommer, J., Schuchardt, J., Bojchevski, A., and Günnemann, S. Generalization of neural combinatorial solvers through the lens of adversarial robustness. In *International Conference on Learning Representations*, 2022. URL <https://openreview.net/forum?id=vJZ7dPIjip3>.
- Gilmer, J., Schoenholz, S. S., Riley, P. F., Vinyals, O., and Dahl, G. E. Neural message passing for quantum chemistry. In *International conference on machine learning*, pp. 1263–1272. PMLR, 2017.
- Gong, S., Li, M., Feng, J., Wu, Z., and Kong, L. Diffuseq: Sequence to sequence text generation with diffusion models. *arXiv preprint arXiv:2210.08933*, 2022.
- Gonzalez, T. F. *Handbook of approximation algorithms and metaheuristics*. Chapman and Hall/CRC, 2007.
- Graikos, A., Malkin, N., Jojic, N., and Samaras, D. Diffusion models as plug-and-play priors. In *Thirty-Sixth Conference on Neural Information Processing Systems*, 2022. URL <https://arxiv.org/pdf/2206.09012.pdf>.
- Gu, J., Bradbury, J., Xiong, C., Li, V. O., and Socher, R. Non-autoregressive neural machine translation. In *International Conference on Learning Representations*, 2018.
- Gu, S., Chen, D., Bao, J., Wen, F., Zhang, B., Chen, D., Yuan, L., and Guo, B. Vector quantized diffusion model for text-to-image synthesis. In *Proceedings of the IEEE/CVF Conference on Computer Vision and Pattern Recognition*, pp. 10696–10706, 2022.
- Gurobi Optimization, L. Gurobi optimizer reference manual, 2018.
- Hamilton, W., Ying, Z., and Leskovec, J. Inductive representation learning on large graphs. *Advances in neural information processing systems*, 30, 2017.
- Han, X., Kumar, S., and Tsvetkov, Y. Ssd-lm: Semi-autoregressive simplex-based diffusion language model for text generation and modular control. *arXiv preprint arXiv:2210.17432*, 2022.
- He, Z., Sun, T., Wang, K., Huang, X., and Qiu, X. Diffusionbert: Improving generative masked language models with diffusion models. *arXiv preprint arXiv:2211.15029*, 2022.
- Helsgaun, K. An extension of the Lin-Kernighan-Helsgaun TSP solver for constrained traveling salesman and vehicle routing problems. Technical report, Roskilde University, 2017.
- Ho, J., Jain, A., and Abbeel, P. Denoising diffusion probabilistic models. *Advances in Neural Information Processing Systems*, 33:6840–6851, 2020.
- Ho, J., Chan, W., Saharia, C., Whang, J., Gao, R., Gritsenko, A., Kingma, D. P., Poole, B., Norouzi, M., Fleet, D. J., et al. Imagen video: High definition video generation with diffusion models. *arXiv preprint arXiv:2210.02303*, 2022a.
- Ho, J., Saharia, C., Chan, W., Fleet, D. J., Norouzi, M., and Salimans, T. Cascaded diffusion models for high fidelity image generation. *J. Mach. Learn. Res.*, 23:47–1, 2022b.
- Ho, J., Salimans, T., Gritsenko, A., Chan, W., Norouzi, M., and Fleet, D. J. Video diffusion models. *arXiv preprint arXiv:2204.03458*, 2022c.
- Hoogetboom, E., Nielsen, D., Jaini, P., Forré, P., and Welling, M. Argmax flows and multinomial diffusion: Learning categorical distributions. *Advances in Neural Information Processing Systems*, 34:12454–12465, 2021.
- Hoogetboom, E., Satorras, V. G., Vignac, C., and Welling, M. Equivariant diffusion for molecule generation in 3d. In *International Conference on Machine Learning*, pp. 8867–8887. PMLR, 2022.

- Hoos, H. H. and Stützle, T. SATLIB: An online resource for research on SAT. *Sat*, 2000:283–292, 2000.
- Hottung, A. and Tierney, K. Neural large neighborhood search for the capacitated vehicle routing problem. *arXiv preprint arXiv:1911.09539*, 2019.
- Hottung, A., Kwon, Y.-D., and Tierney, K. Efficient active search for combinatorial optimization problems. *arXiv preprint arXiv:2106.05126*, 2021.
- Hudson, B., Li, Q., Malencia, M., and Prorok, A. Graph neural network guided local search for the traveling salesperson problem. In *International Conference on Learning Representations*, 2022. URL <https://openreview.net/forum?id=ar92oEosBIg>.
- Ioffe, S. and Szegedy, C. Batch normalization: Accelerating deep network training by reducing internal covariate shift. In *International conference on machine learning*, pp. 448–456. PMLR, 2015.
- Johnson, D. D., Austin, J., Berg, R. v. d., and Tarlow, D. Beyond in-place corruption: Insertion and deletion in denoising probabilistic models. *arXiv preprint arXiv:2107.07675*, 2021.
- Joshi, C. K., Laurent, T., and Bresson, X. An efficient graph convolutional network technique for the travelling salesman problem. *arXiv preprint arXiv:1906.01227*, 2019.
- Joshi, C. K., Cappart, Q., Rousseau, L.-M., and Laurent, T. Learning the travelling salesperson problem requires rethinking generalization. *Constraints*, pp. 1–29, 2022.
- Karalias, N. and Loukas, A. Erdos goes neural: an unsupervised learning framework for combinatorial optimization on graphs. *Advances in Neural Information Processing Systems*, 33:6659–6672, 2020.
- Karras, T., Aittala, M., Aila, T., and Laine, S. Elucidating the design space of diffusion-based generative models. *arXiv preprint arXiv:2206.00364*, 2022.
- Khalil, E., Dai, H., Zhang, Y., Dilkina, B., and Song, L. Learning combinatorial optimization algorithms over graphs. *Advances in neural information processing systems*, 30, 2017.
- Kim, M., Park, J., et al. Learning collaborative policies to solve NP-hard routing problems. *Advances in Neural Information Processing Systems*, 34, 2021.
- Kim, M., Park, J., and Park, J. Sym-NCO: Leveraging symmetry for neural combinatorial optimization. In Oh, A. H., Agarwal, A., Belgrave, D., and Cho, K. (eds.), *Advances in Neural Information Processing Systems*, 2022. URL <https://openreview.net/forum?id=kHrE2vi5Rvs>.
- Kingma, D., Salimans, T., Poole, B., and Ho, J. Variational diffusion models. *Advances in neural information processing systems*, 34:21696–21707, 2021.
- Kipf, T. N. and Welling, M. Semi-supervised classification with graph convolutional networks. *arXiv preprint arXiv:1609.02907*, 2016.
- Kipf, T. N. and Welling, M. Semi-supervised classification with graph convolutional networks. In *International Conference on Learning Representations*, 2017. URL <https://openreview.net/forum?id=SJU4ayYgl>.
- Konda, V. R. and Tsitsiklis, J. N. Actor-critic algorithms. In *Advances in neural information processing systems*, pp. 1008–1014, 2000.
- Kool, W., van Hoof, H., and Welling, M. Attention, learn to solve routing problems! In *International Conference on Learning Representations*, 2019a.
- Kool, W., van Hoof, H., and Welling, M. Buy 4 REINFORCE samples, get a baseline for free! In *Deep Reinforcement Learning Meets Structured Prediction, ICLR 2019 Workshop*, 2019b.
- Krizhevsky, A. and Hinton, G. Convolutional deep belief networks on cifar-10. *Unpublished manuscript*, 40(7): 1–9, 2010.
- Kwon, Y.-D., Choo, J., Kim, B., Yoon, I., Gwon, Y., and Min, S. POMO: Policy optimization with multiple optima for reinforcement learning. *arXiv preprint arXiv:2010.16011*, 2020.
- Kwon, Y.-D., Choo, J., Yoon, I., Park, M., Park, D., and Gwon, Y. Matrix encoding networks for neural combinatorial optimization. *Advances in Neural Information Processing Systems*, 34, 2021.
- Li, X. L., Thickstun, J., Gulrajani, I., Liang, P., and Hashimoto, T. Diffusion-LM improves controllable text generation. In Oh, A. H., Agarwal, A., Belgrave, D., and Cho, K. (eds.), *Advances in Neural Information Processing Systems*, 2022. URL <https://openreview.net/forum?id=3s9IrEsjLyk>.
- Li, Z., Chen, Q., and Koltun, V. Combinatorial optimization with graph convolutional networks and guided tree search. *Advances in neural information processing systems*, 31, 2018.
- Lin, S. and Kernighan, B. W. An effective heuristic algorithm for the traveling-salesman problem. *Operations research*, 21(2):498–516, 1973.

- Liu, J., Li, C., Ren, Y., Chen, F., and Zhao, Z. Diffsinger: Singing voice synthesis via shallow diffusion mechanism. In *Proceedings of the AAAI Conference on Artificial Intelligence*, volume 36, pp. 11020–11028, 2022.
- Liu, L., Ren, Y., Lin, Z., and Zhao, Z. Pseudo numerical methods for diffusion models on manifolds. In *International Conference on Learning Representations*, 2021.
- Lu, C., Zhou, Y., Bao, F., Chen, J., Li, C., and Zhu, J. Dpm-solver: A fast ode solver for diffusion probabilistic model sampling in around 10 steps. *arXiv preprint arXiv:2206.00927*, 2022a.
- Lu, C., Zhou, Y., Bao, F., Chen, J., Li, C., and Zhu, J. Dpm-solver++: Fast solver for guided sampling of diffusion probabilistic models. *arXiv preprint arXiv:2211.01095*, 2022b.
- Lu, H., Zhang, X., and Yang, S. A learning-based iterative method for solving vehicle routing problems. In *International Conference on Learning Representations*, 2020.
- Luo, S., Su, Y., Peng, X., Wang, S., Peng, J., and Ma, J. Antigen-specific antibody design and optimization with diffusion-based generative models for protein structures. In Oh, A. H., Agarwal, A., Belgrave, D., and Cho, K. (eds.), *Advances in Neural Information Processing Systems*, 2022. URL <https://openreview.net/forum?id=jSorGn2Tjg>.
- Ma, Q., Ge, S., He, D., Thaker, D., and Drori, I. Combinatorial optimization by graph pointer networks and hierarchical reinforcement learning. *arXiv preprint arXiv:1911.04936*, 2019.
- Ma, Y., Li, J., Cao, Z., Song, W., Zhang, L., Chen, Z., and Tang, J. Learning to iteratively solve routing problems with dual-aspect collaborative transformer. *Advances in Neural Information Processing Systems*, 34:11096–11107, 2021.
- Malherbe, C., Grosnit, A., Tutunov, R., Ammar, H. B., and Wang, J. Optimistic tree searches for combinatorial black-box optimization. In Oh, A. H., Agarwal, A., Belgrave, D., and Cho, K. (eds.), *Advances in Neural Information Processing Systems*, 2022. URL <https://openreview.net/forum?id=JGLW4DvX11F>.
- Meng, C., Song, Y., Song, J., Wu, J., Zhu, J.-Y., and Ermon, S. Sdedit: Image synthesis and editing with stochastic differential equations. *arXiv preprint arXiv:2108.01073*, 2021.
- Nair, V., Bartunov, S., Gimeno, F., von Glehn, I., Li-chocki, P., Lobov, I., O’Donoghue, B., Sonnerat, N., Tjandraatmadja, C., Wang, P., et al. Solving mixed integer programs using neural networks. *arXiv preprint arXiv:2012.13349*, 2020.
- Nazari, M., Oroojlooy, A., Snyder, L., and Takác, M. Reinforcement learning for solving the vehicle routing problem. *Advances in neural information processing systems*, 31, 2018.
- Nichol, A., Dhariwal, P., Ramesh, A., Shyam, P., Mishkin, P., McGrew, B., Sutskever, I., and Chen, M. Glide: Towards photorealistic image generation and editing with text-guided diffusion models. *arXiv preprint arXiv:2112.10741*, 2021.
- Nichol, A. Q. and Dhariwal, P. Improved denoising diffusion probabilistic models. In *International Conference on Machine Learning*, pp. 8162–8171. PMLR, 2021.
- Niu, C., Song, Y., Song, J., Zhao, S., Grover, A., and Ermon, S. Permutation invariant graph generation via score-based generative modeling. In *International Conference on Artificial Intelligence and Statistics*, pp. 4474–4484. PMLR, 2020.
- Ouyang, W., Wang, Y., Han, S., Jin, Z., and Weng, P. Improving generalization of deep reinforcement learning-based tsp solvers. *arXiv preprint arXiv:2110.02843*, 2021.
- Papadimitriou, C. H. and Steiglitz, K. *Combinatorial optimization: algorithms and complexity*. Courier Corporation, 1998.
- Park, J., Chun, J., Kim, S. H., Kim, Y., and Park, J. Learning to schedule job-shop problems: representation and policy learning using graph neural network and reinforcement learning. *International Journal of Production Research*, 59(11):3360–3377, 2021.
- Peng, B., Wang, J., and Zhang, Z. A deep reinforcement learning algorithm using dynamic attention model for vehicle routing problems. In *International Symposium on Intelligence Computation and Applications*, pp. 636–650. Springer, 2019.
- Qiu, R., Sun, Z., and Yang, Y. Dimes: A differentiable meta solver for combinatorial optimization problems. In *Advances in Neural Information Processing Systems*, 2022.
- Ramesh, A., Dhariwal, P., Nichol, A., Chu, C., and Chen, M. Hierarchical text-conditional image generation with clip latents. *arXiv preprint arXiv:2204.06125*, 2022.
- Rombach, R., Blattmann, A., Lorenz, D., Esser, P., and Ommer, B. High-resolution image synthesis with latent diffusion models. In *Proceedings of the IEEE/CVF Conference on Computer Vision and Pattern Recognition*, pp. 10684–10695, 2022.

- Saharia, C., Chan, W., Chang, H., Lee, C., Ho, J., Salimans, T., Fleet, D., and Norouzi, M. Palette: Image-to-image diffusion models. In *ACM SIGGRAPH 2022 Conference Proceedings*, pp. 1–10, 2022a.
- Saharia, C., Chan, W., Saxena, S., Li, L., Whang, J., Denton, E., Ghasemipour, S. K. S., Ayan, B. K., Mahdavi, S. S., Lopes, R. G., et al. Photorealistic text-to-image diffusion models with deep language understanding. *arXiv preprint arXiv:2205.11487*, 2022b.
- Shaw, P. A new local search algorithm providing high quality solutions to vehicle routing problems. *APES Group, Dept of Computer Science, University of Strathclyde, Glasgow, Scotland, UK*, 46, 1997.
- Silver, D., Huang, A., Maddison, C. J., Guez, A., Sifre, L., Van Den Driessche, G., Schrittwieser, J., Antonoglou, I., Panneershelvam, V., Lanctot, M., et al. Mastering the game of go with deep neural networks and tree search. *nature*, 529(7587):484–489, 2016.
- Singer, U., Polyak, A., Hayes, T., Yin, X., An, J., Zhang, S., Hu, Q., Yang, H., Ashual, O., Gafni, O., et al. Make-a-video: Text-to-video generation without text-video data. *arXiv preprint arXiv:2209.14792*, 2022.
- Sohl-Dickstein, J., Weiss, E., Maheswaranathan, N., and Ganguli, S. Deep unsupervised learning using nonequilibrium thermodynamics. In *International Conference on Machine Learning*, pp. 2256–2265. PMLR, 2015.
- Song, J., Meng, C., and Ermon, S. Denoising diffusion implicit models. In *International Conference on Learning Representations*, 2021a. URL <https://openreview.net/forum?id=StlgIarCHLP>.
- Song, Y. and Ermon, S. Generative modeling by estimating gradients of the data distribution. *Advances in Neural Information Processing Systems*, 32, 2019.
- Song, Y. and Ermon, S. Improved techniques for training score-based generative models. *Advances in neural information processing systems*, 33:12438–12448, 2020.
- Song, Y., Sohl-Dickstein, J., Kingma, D. P., Kumar, A., Ermon, S., and Poole, B. Score-based generative modeling through stochastic differential equations. In *International Conference on Learning Representations*, 2021b.
- Sun, H., Yu, L., Dai, B., Schuurmans, D., and Dai, H. Score-based continuous-time discrete diffusion models. *arXiv preprint arXiv:2211.16750*, 2022.
- Vaswani, A., Shazeer, N., Parmar, N., Uszkoreit, J., Jones, L., Gomez, A. N., Kaiser, Ł., and Polosukhin, I. Attention is all you need. In *Advances in neural information processing systems*, pp. 5998–6008, 2017.
- Veličković, P., Cucurull, G., Casanova, A., Romero, A., Liò, P., and Bengio, Y. Graph attention networks. In *International Conference on Learning Representations*, 2018.
- Vignac, C., Krawczuk, I., Siraudin, A., Wang, B., Cevher, V., and Frossard, P. Digress: Discrete denoising diffusion for graph generation. *arXiv preprint arXiv:2209.14734*, 2022.
- Wang, C., Yang, Y., Slumbers, O., Han, C., Guo, T., Zhang, H., and Wang, J. A game-theoretic approach for improving generalization ability of TSP solvers. *arXiv preprint arXiv:2110.15105*, 2021a.
- Wang, R., Hua, Z., Liu, G., Zhang, J., Yan, J., Qi, F., Yang, S., Zhou, J., and Yang, X. A bi-level framework for learning to solve combinatorial optimization on graphs. *arXiv preprint arXiv:2106.04927*, 2021b.
- Williams, R. J. Simple statistical gradient-following algorithms for connectionist reinforcement learning. *Machine learning*, 8(3):229–256, 1992.
- Wu, L., Gong, C., Liu, X., Ye, M., and Liu, Q. Diffusion-based molecule generation with informative prior bridges. *arXiv preprint arXiv:2209.00865*, 2022.
- Wu, Y., Song, W., Cao, Z., Zhang, J., and Lim, A. Learning improvement heuristics for solving routing problems.. *IEEE transactions on neural networks and learning systems*, 2021.
- Xin, L., Song, W., Cao, Z., and Zhang, J. Multi-decoder attention model with embedding glimpse for solving vehicle routing problems. In *Proceedings of the AAAI Conference on Artificial Intelligence*, volume 35, pp. 12042–12049, 2021a.
- Xin, L., Song, W., Cao, Z., and Zhang, J. NeuroLKH: Combining deep learning model with Lin–Kernighan–Helsgaun heuristic for solving the traveling salesman problem. *Advances in Neural Information Processing Systems*, 34, 2021b.
- Xu, K., Hu, W., Leskovec, J., and Jegelka, S. How powerful are graph neural networks? In *International Conference on Learning Representations*, 2019. URL <https://openreview.net/forum?id=ryGs6iA5Km>.
- Xu, M., Yu, L., Song, Y., Shi, C., Ermon, S., and Tang, J. Geodiff: A geometric diffusion model for molecular conformation generation. In *International Conference on Learning Representations*, 2021.
- Yang, D., Yu, J., Wang, H., Wang, W., Weng, C., Zou, Y., and Yu, D. Diffsound: Discrete diffusion model for text-to-sound generation. *arXiv preprint arXiv:2207.09983*, 2022.

- Yolcu, E. and Póczos, B. Learning local search heuristics for boolean satisfiability. In *NeurIPS*, pp. 7990–8001, 2019.
- Yu, J., Xu, Y., Koh, J. Y., Luong, T., Baid, G., Wang, Z., Vasudevan, V., Ku, A., Yang, Y., Ayan, B. K., et al. Scaling autoregressive models for content-rich text-to-image generation. *Transactions on Machine Learning Research*.
- Yu, L., Cheng, Y., Sohn, K., Lezama, J., Zhang, H., Chang, H., Hauptmann, A. G., Yang, M.-H., Hao, Y., Essa, I., et al. Magvit: Masked generative video transformer. *arXiv preprint arXiv:2212.05199*, 2022.
- Zhang, C., Song, W., Cao, Z., Zhang, J., Tan, P. S., and Xu, C. Learning to dispatch for job shop scheduling via deep reinforcement learning. *arXiv preprint arXiv:2010.12367*, 2020.

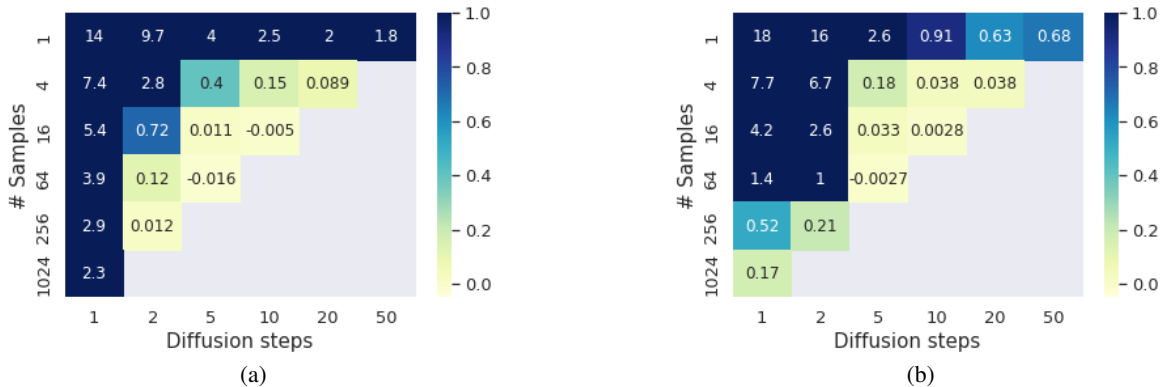


Figure 4: The performance Drop (%) of continuous diffusion (a) and discrete diffusion (b) models on TSP-50 with different diffusion steps and number of samples. (c): The results are reported with greedy decoding without 2-opt post-processing.

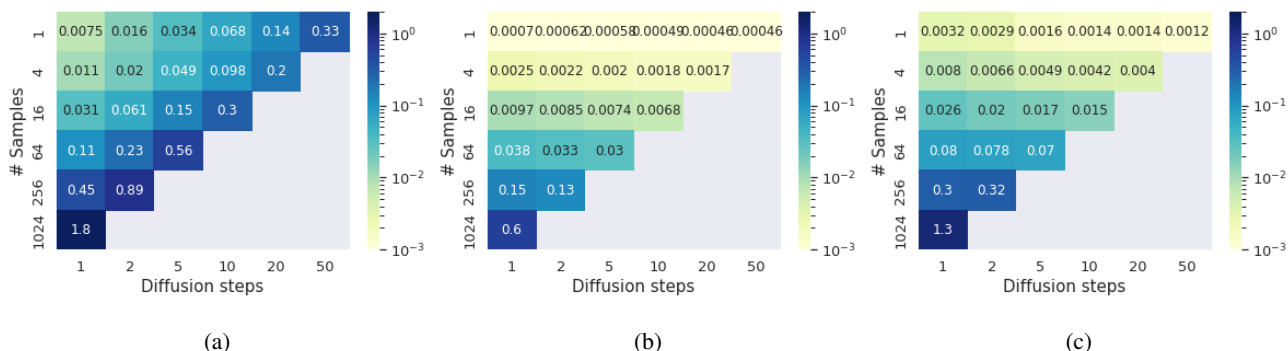


Figure 5: The inference per-instance run-time (sec) of diffusion models on TSP-50, where the total run-time is decomposed to neural network (a) + greedy decoding (b) + 2-opt (c).

A. Additional Related Work

Autoregressive Constructive Solvers Since Bello et al. (2016) proposed the first autoregressive CO solver, more advanced models have been developed in the years since (Deudon et al., 2018; Kool et al., 2019a; Peng et al., 2019; Drori et al., 2020; Kwon et al., 2021), including better network backbones (Vaswani et al., 2017; Kool et al., 2019a; Bresson & Laurent, 2018)), more advanced deep reinforcement learning algorithms (Khalil et al., 2017; Ma et al., 2019; Kool et al., 2019b; Kwon et al., 2020; Ouyang et al., 2021; Xin et al., 2021a; Wang et al., 2021a; Choo et al., 2022), improved training strategies (Kim et al., 2022; Bi et al., 2022), and for a wider range of NPC problems such as Capacitated Vehicle Routing Problem (CVRP) (Nazari et al., 2018), Job Shop Scheduling Problem (JSSP) (Zhang et al., 2020; Park et al., 2021), Maximal Independent Set (MIS) problem (Khalil et al., 2017; Ahn et al., 2020; Malherbe et al., 2022; Qiu et al., 2022), and boolean satisfiability problem (SAT) (Yolcu & Póczos, 2019).

Improvement Heuristics Solvers Unlike construction heuristics, DRL-based improvement heuristics solvers use neural networks to iteratively enhance the quality of the current solution until the computational budget is exhausted. Such DRL-based improvement heuristics methods are usually inspired by classical local search algorithms such as 2-opt (Croes, 1958) and the large neighborhood search (LNS) (Shaw, 1997), and have been demonstrated with outstanding results by many previous works (Chen & Tian, 2019; Hottung & Tierney, 2019; da Costa et al., 2020; d O Costa et al., 2020; Xin et al., 2021b; Ma et al., 2021; Wu et al., 2021; Lu et al., 2020; Wang et al., 2021b; Kim et al., 2021; Hudson et al., 2022).

Improvement heuristics methods, while showing superior performance compared to construction heuristics methods, come at the cost of increased computational time, often requiring thousands of actions even for small-scale problems with hundreds of nodes (d O Costa et al., 2020; Wang et al., 2021b). This is due to the sequential application of local operations, such as 2-opt, on existing solutions, resulting in a bottleneck for latency. On the other hand, DIFUSCO has the advantage of denoising all variables in parallel, which leads to a reduction in the number of network evaluations required.

Graph-based Diffusion Solvers for Combinatorial Optimization

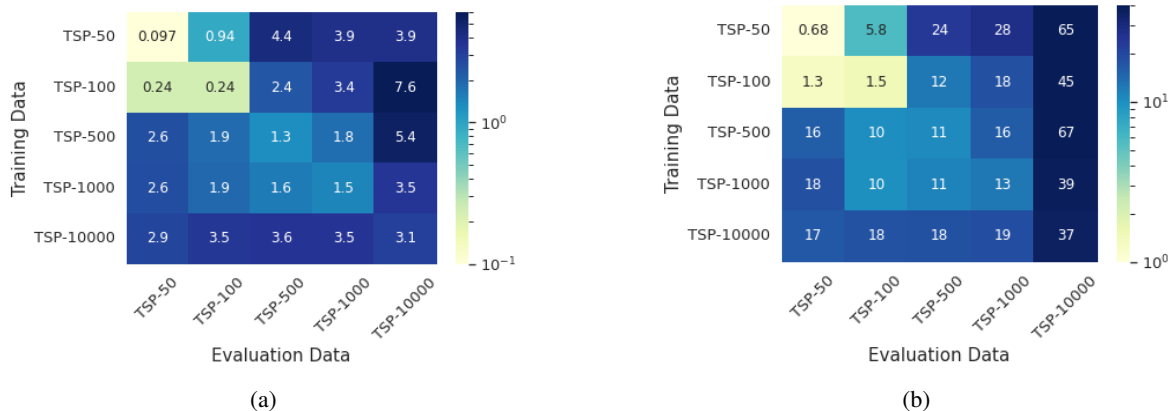


Figure 6: Generalization tests of discrete DIFUSCO trained and evaluated on TSP problems across various scales. The results are reported with (a) and without (b) 2-opt post-processing.

Table 4: Comparing discrete diffusion and continuous diffusion on TSP-100 with various diffusion steps and number of parallel sampling. cosine schedule is used for fast sampling.

DIFFUSION STEPS	#SAMPLE	DISCRETE DIFFUSION (Drop%)		CONTINUOUS DIFFUSION (Drop%)		PER-INSTANCE RUNTIME (sec)		
		w/ 2OPT	w/o 2OPT	w/ 2OPT	w/o 2OPT	NN	GD	2-OPT
50	1	0.23869	1.45574	1.46146	7.66379	0.50633	0.00171	0.00210
100	1	0.23366	1.48161	1.32573	7.02117	1.00762	0.00170	0.00207
50	4	0.02253	0.09280	0.42741	1.65264	1.52401	0.00643	0.00575
10	16	-0.01870	0.00519	0.13015	0.54983	1.12550	0.02581	0.02228
50	16	-0.02322	-0.00699	0.09407	0.30712	5.63712	0.02525	0.02037

Continuous Diffusion Models Diffusion models were first proposed by Sohl-Dickstein et al. (2015) and recently achieved impressive success on various tasks, such as high-resolution image synthesis (Dhariwal & Nichol, 2021; Ho et al., 2022b), image editing (Meng et al., 2021; Saharia et al., 2022a), text-to-image generation (Nichol et al., 2021; Saharia et al., 2022b; Rombach et al., 2022; Ramesh et al., 2022; Gu et al., 2022), waveform generation (Chen et al., 2020; 2021; Liu et al., 2022), video generation (Ho et al., 2022c;a; Singer et al., 2022), and molecule generation (Xu et al., 2021; Hoogeboom et al., 2022; Wu et al., 2022).

Recent works have also drawn connections to stochastic differential equations (SDEs) (Song et al., 2021b) and ordinary differential equations (ODEs) (Song et al., 2021a) in a continuous time framework, leading to improved sampling algorithms by solving discretized SDEs/ODEs with higher-order solvers (Liu et al., 2021; Lu et al., 2022b;a) or implicit diffusion (Song et al., 2021a).

B. Additional Results

Discrete Diffusion v.s. Continuous Diffusion on TSP-100 We also compare discrete diffusion and continuous diffusion on the TSP-100 benchmark and report the results in Tab. 4. We can see that on TSP-100, discrete diffusion models still consistently outperform their continuous counterparts in various settings.

More Diffusion Steps v.s. More Sampling (w/o 2-opt) Fig. 4 report the results of continuous diffusion and discrete diffusion with various diffusion steps and numbers of parallel sampling, without using 2-opt post-processing. The cosine denoising schedule is used for fast inference. Again, we find that discrete diffusion outperforms continuous diffusion across various settings.

Besides, we find that without the 2-opt post-processing, performing more diffusion iterations is much more effective than sampling more solutions, even when the former uses less computation. For example, 20 (diffusion steps) \times 4 (samples) not only significantly outperforms 1 (diffusion steps) \times 1024 (samples), but also has a 18.5 \times less runtime.

Runtime Analysis We report the decomposed runtime (neural network + greedy decoding + 2-opt) for diffusion models on TSP-50 in Fig. 5. We can see that while neural network execution takes the majority of total runtime, 2-opt also takes a non-negligible portion of the runtime, especially when only a few diffusion steps (like 1 or 2) are used.

Generalization Tests (w/o 2opt) We also report the generalization tests of discrete DIFUSCO without 2-opt post-processing in Fig.6 (b).

C. Discussion on the $\{0, 1\}^N$ Vector Space of CO Problems

The design of the $\{0, 1\}^N$ vector space can also represent non-graph-based NP-complete combinatorial optimization problems. For example, on the more general Mixed Integer Programming (MIP) problem, we can let \mathcal{X}_s be a 0/1 indication set of all extended variables³. $\text{cost}(\cdot)$ can be defined as a linear/quadratic function of \mathbf{x} , and $\text{valid}(\cdot)$ is a function validating all linear/quadratic constraints, bound constraints, and integrality constraints.

D. Additional Experiment Details

Metrics: TSP For TSP, Length is defined as the average length of the system-predicted tour for each test-set instance. Drop is the average of the relative decrease in performance compared to a baseline method. Time is the total clock time required to generate solutions for all test instances, and is presented in seconds (s), minutes (m), or hours (h).

Metrics: MIS For MIS, Size (the larger, the better) is the average size of the system-predicted maximal independent set for each test-set graph, Drop and Time are defined similarly as in the TSP case.

Hardware All the methods are trained with $8 \times$ NVIDIA Tesla V100 Volta GPUs and evaluated on a single NVIDIA Tesla V100 Volta GPU, with $40 \times$ Intel(R) Xeon(R) Gold 6248 CPUs @ 2.50GHz.

Random Seeds Since the diffusion models can generate an arbitrary sample from its distribution even with the greedy decoding scheme, we report the averaged results across 5 different random seeds when reporting all results.

Training Details All DIFUSCO models are trained with a cosine learning rate schedule starting from $2e-4$ and ending at 0.

- TSP-50: We use 1502000 random instances and train DIFUSCO for 50 epochs with a batch size of 512.
- TSP-100: We use 1502000 random instances and train DIFUSCO for 50 epochs with a batch size of 256.
- TSP-500: We use 128000 random instances and train DIFUSCO for 50 epochs with a batch size of 64. We also apply curriculum learning and initialize the model from the TSP-100 checkpoint.
- TSP-1000: We use 64000 random instances and train DIFUSCO for 50 epochs with a batch size of 64. We also apply curriculum learning and initialize the model from the TSP-100 checkpoint.
- TSP-10000: We use 6400 random instances and train DIFUSCO for 50 epochs with a batch size of 8. We also apply curriculum learning and initialize the model from the TSP-500 checkpoint.
- SATLIB: We use the training split of 49500 examples from (Hoos & Stützle, 2000; Qiu et al., 2022) and train DIFUSCO for 50 epochs with a batch size of 128.
- ER-[700-800]: We use 163840 random instances and train DIFUSCO for 50 epochs with a batch size of 32.

E. Decoding Strategies

Greedy Decoding We use a simple greedy decoding scheme for diffusion models, where we sample one solution from the learned distribution $p_\theta(\mathbf{x}_0)$. We compare this scheme with other autoregressive constructive solvers that also use greedy decoding.

Sampling Following Kool et al. (2019a), we also use a sampling scheme where we sample multiple solutions in parallel (i.e., each diffusion model starts with a different noise \mathbf{x}_T) and report the best one.

³For an integer variable z that can be assigned values from a finite set with cardinality $\text{card}(z)$, any target value can be represented as a sequence of $\lceil \log_2(\text{card}(z)) \rceil$ bits (Nair et al., 2020; Chen et al., 2022).

Monte Carlo Tree Search For the TSP task, we adopt a more advanced reinforcement learning-based search approach, i.e., Monte Carlo tree search (MCTS), to find high-quality solutions. In MCTS, we sample k -opt transformation actions guided by the heatmap generated by the diffusion model to improve the current solutions. The MCTS repeats the simulation, selection, and back-propagation steps until no improving actions are found in the sampling pool. For more details, please refer to (Fu et al., 2021).

F. Fast Inference for Continuous and Discrete Diffusion Models

We first describe the denoising diffusion implicit models (DDIMs) (Song et al., 2021a) algorithm for accelerating inference for continuous diffusion models.

Formally, consider the forward process defined not on all the latent variables $\mathbf{x}_{1:T}$, but on a subset $\{\mathbf{x}_{\tau_1}, \dots, \mathbf{x}_{\tau_M}\}$, where τ is an increasing sub-sequence of $[1, \dots, T]$ with length M , $\mathbf{x}_{\tau_1} = \mathbf{1}$ and $\mathbf{x}_{\tau_M} = \mathbf{T}$.

For continuous diffusion, the marginal can still be defined as:

$$q(\mathbf{x}_{\tau_i} | \mathbf{x}_0) := \mathcal{N}(\mathbf{x}_{\tau_i}; \sqrt{\bar{\alpha}_{\tau_i}} \mathbf{x}_0, (1 - \bar{\alpha}_{\tau_i}) \mathbf{I}) \quad (15)$$

And it's (deterministic) posterior is defined by:

$$q(\mathbf{x}_{\tau_{i-1}} | \mathbf{x}_{\tau_i}, \mathbf{x}_0) := \mathcal{N}(\mathbf{x}_{\tau_{i-1}}; \sqrt{\frac{\bar{\alpha}_{\tau_{i-1}}}{\bar{\alpha}_{\tau_i}}} \left(\mathbf{x}_{\tau_i} - \sqrt{1 - \bar{\alpha}_{\tau_i}} \cdot \tilde{\epsilon}_{\tau_i} \right) + \sqrt{1 - \bar{\alpha}_{\tau_{i-1}}} \cdot \tilde{\epsilon}_{\tau_i}, \mathbf{0}) \quad (16)$$

where $\tilde{\epsilon}_{\tau_i} = (\mathbf{x}_{\tau_i} - \sqrt{\bar{\alpha}_{\tau_i}} \mathbf{x}_0) / \sqrt{1 - \bar{\alpha}_{\tau_i}}$ is the (predicted) diffusion noise.

Next, we describe its analogy in the discrete domain, which is first proposed by Austin et al. (2021).

For discrete diffusion, the marginal can still be defined as:

$$q(\mathbf{x}_{\tau_i} | \mathbf{x}_0) = \text{Cat}(\mathbf{x}_{\tau_i}; \mathbf{p} = \mathbf{x}_0 \bar{\mathbf{Q}}_{\tau_i}), \quad (17)$$

while the posterior becomes:

$$\begin{aligned} q(\mathbf{x}_{\tau_{i-1}} | \mathbf{x}_{\tau_i}, \mathbf{x}_0) &= \frac{q(\mathbf{x}_{\tau_i} | \mathbf{x}_{\tau_{i-1}}, \mathbf{x}_0) q(\mathbf{x}_{\tau_{i-1}} | \mathbf{x}_0)}{q(\mathbf{x}_{\tau_i} | \mathbf{x}_0)} \\ &= \text{Cat} \left(\mathbf{x}_{\tau_{i-1}}; \mathbf{p} = \frac{\mathbf{x}_{\tau_i} \bar{\mathbf{Q}}_{\tau_{i-1}, \tau_i}^\top \odot \mathbf{x}_0 \bar{\mathbf{Q}}_{\tau_{i-1}}}{\mathbf{x}_0 \bar{\mathbf{Q}}_{\tau_i} \mathbf{x}_{\tau_i}^\top} \right), \end{aligned} \quad (18)$$

where $\bar{\mathbf{Q}}_{t', t} = \mathbf{Q}_{t'+1} \dots \mathbf{Q}_t$.

G. Neural Network Architecture

We adopt an anisotropic graph neural network with edge gating mechanisms (Bresson & Laurent, 2018; Joshi et al., 2022) as the backbone network for both discrete and continuous diffusion models.

Anisotropic Graph Neural Networks Let \mathbf{h}_i^ℓ and e_{ij}^ℓ denote the node and edge features at layer ℓ associated with node i and edge ij , respectively. \mathbf{t} is the sinusoidal features (Vaswani et al., 2017) of denoising timestep t . The features at the next layer is propagated with an anisotropic message passing scheme:

$$\begin{aligned} \hat{e}_{ij}^{\ell+1} &= \mathbf{P}^\ell e_{ij}^\ell + \mathbf{Q}^\ell \mathbf{h}_i^\ell + \mathbf{R}^\ell \mathbf{h}_j^\ell, \\ e_{ij}^{\ell+1} &= e_{ij}^\ell + \text{MLP}_e(\text{BN}(\hat{e}_{ij}^{\ell+1})) + \text{MLP}_t(\mathbf{t}), \\ \mathbf{h}_i^{\ell+1} &= \mathbf{h}_i^\ell + \alpha(\text{BN}(\mathbf{U}^\ell \mathbf{h}_i^\ell + \mathcal{A}_{j \in \mathcal{N}_i}(\sigma(\hat{e}_{ij}^{\ell+1}) \odot \mathbf{V}^\ell \mathbf{h}_j^\ell))), \end{aligned}$$

where $\mathbf{U}^\ell, \mathbf{V}^\ell, \mathbf{P}^\ell, \mathbf{Q}^\ell, \mathbf{R}^\ell \in \mathbb{R}^{d \times d}$ are the learnable parameters of layer ℓ , α denotes the ReLU (Krizhevsky & Hinton, 2010) activation, BN denotes the Batch Normalization operator (Ioffe & Szegedy, 2015), \mathcal{A} denotes the aggregation function

SUM pooling (Xu et al., 2019), σ is the sigmoid function, \odot is the Hadamard product, \mathcal{N}_i denotes the neighborhoods of node i , and $\text{MLP}_{(\cdot)}$ denotes a 2-layer multi-layer perceptron.

For TSP, e_{ij}^0 are initialized as the corresponding values in \mathbf{x}_t , and \mathbf{h}_i^0 are initialized as sinusoidal features of the nodes. For MIS, e_{ij}^0 are initialized as zeros, and \mathbf{h}_i^0 are initialized as the corresponding values in \mathbf{x}_t . A 2-neuron and 1-neuron classification/regression head is applied to the final embeddings of \mathbf{x}_t ($\{e_{ij}\}$ for edges and $\{\mathbf{h}_i\}$ for nodes) for discrete and continuous diffusion models, respectively.

Hyper-parameters For all TSP and MIS benchmarks, we use a 12-layer Anisotropic GNN with a width of 256 as described above.

H. Experiment Baselines

TSP-50/100 We evaluate DIFUSCO on TSP-50 and TSP-100 against 10 baselines, which belong to two categories: traditional Operations Research (OR) methods and learning-based methods.

- Traditional OR methods include Concorde (Applegate et al., 2006), an exact solver, and 2-opt (Lin & Kernighan, 1973), a heuristic method.
- Learning-based methods include AM (Kool et al., 2019a), GCN (Joshi et al., 2019), Transformer (Bresson & Laurent, 2021), POMO (Kwon et al., 2020), Sym-NCO (Kim et al., 2022), DPDP (Ma et al., 2021), Image Diffusion (Graikos et al., 2022), and MDAM (Xin et al., 2021a). These are the state-of-the-art methods in recent benchmark studies.

TSP-500/1000/10000 We compare DIFUSCO on large-scale TSP problems with 9 baseline methods, which fall into two categories: traditional Operations Research (OR) methods and learning-based methods.

- Traditional OR methods include Concorde (Applegate et al., 2006) and Gurobi (Gurobi Optimization, 2018), which are exact solvers, and LKH-3 (Helsgaun, 2017), which is a strong heuristic solver. We use two settings for LKH-3: (i) *default*: 10000 trials (the default configuration of LKH-3); (ii) *less trials*: 500 trials for TSP-500/1000 and 250 trials for TSP-10000. We also include Farthest Insertion, a simple heuristic method, as a baseline.
- Learning-based methods include EAN (Deudon et al., 2018), AM (Kool et al., 2019a), GCN (Joshi et al., 2019), POMO+EAS (Kwon et al., 2020; Hottung et al., 2021), Att-GCN (Fu et al., 2021), and DIMES (Qiu et al., 2022). These are the state-of-the-art methods in recent benchmark studies. They can be further divided into reinforcement learning (RL) and supervised learning (SL) methods. Some RL methods can also use an Active Search (AS) stage (Bello et al., 2016) to fine-tune each instance. We take the results of the baselines from Fu et al. (2021) and Qiu et al. (2022). Note that except for Att-GCN and DIMES, the baselines are trained on small graphs and tested on large graphs.

MIS For MIS, we compare DIFUSCO with 6 other MIS solvers on the same test sets, including two traditional OR methods (i.e., Gurobi and KaMIS) and four learning-based methods. Gurobi solves MIS as an integer linear program, while KaMIS is a heuristics solver for MIS. The four learning-based methods can be divided into the reinforcement learning (RL) category, i.e., LwD (Ahn et al., 2020) and DIMES (Qiu et al., 2022), and the supervised learning (SL) category, i.e., Intel (Li et al., 2018) and DGL (Böther et al., 2022).

Graph-based Diffusion Solvers for Combinatorial Optimization

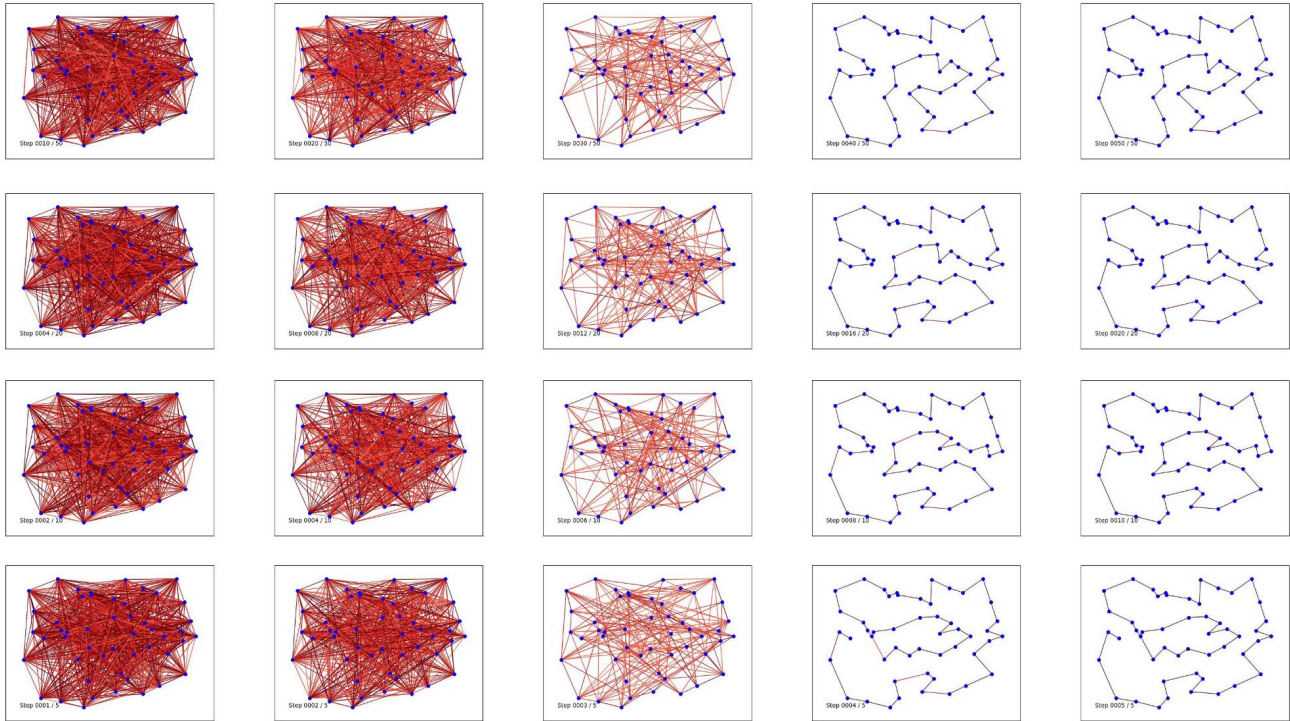


Figure 7: Qualitative illustration of how diffusion steps affect the generation quality of **continuous** diffusion models. The results are reported without any post-processing. **Continuous** DIFUSCO with 50 (first row), 20 (second row), 10 (third row), and 5 (last row) diffusion steps in *cosine* schedule are shown.

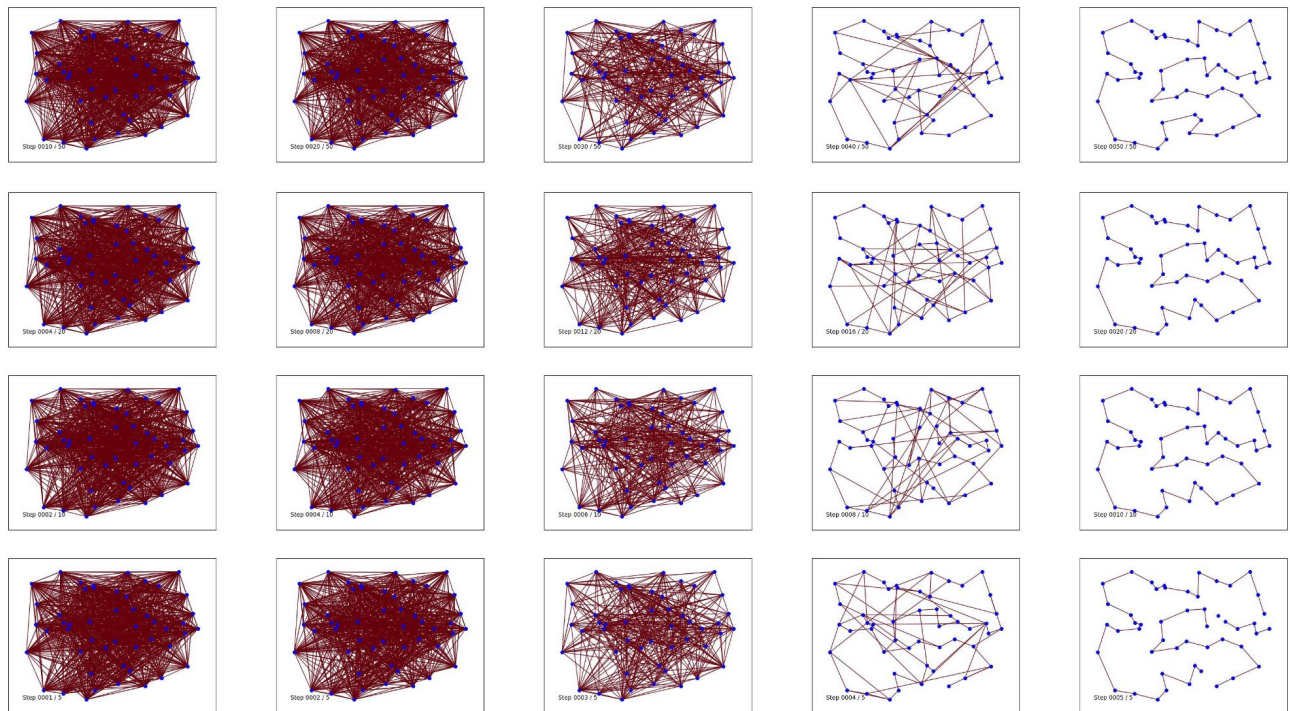


Figure 8: Qualitative illustration of how diffusion steps affect the generation quality of **discrete** diffusion models. The results are reported without any post-processing. **Discrete** DIFUSCO with 50 (first row), 20 (second row), 10 (third row), and 5 (last row) diffusion steps in *cosine* schedule are shown.

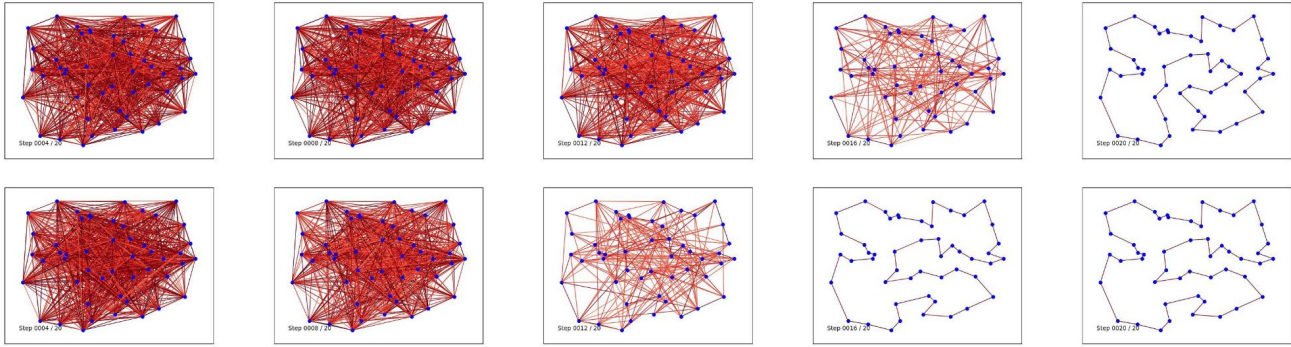


Figure 9: Qualitative illustration of how diffusion schedules affect the generation quality of **continuous** diffusion models. The results are reported without any post-processing. **Continuous** DIFUSCO with `linear` schedule (first row) and `cosine` schedule (second row) with 20 diffusion steps are shown.

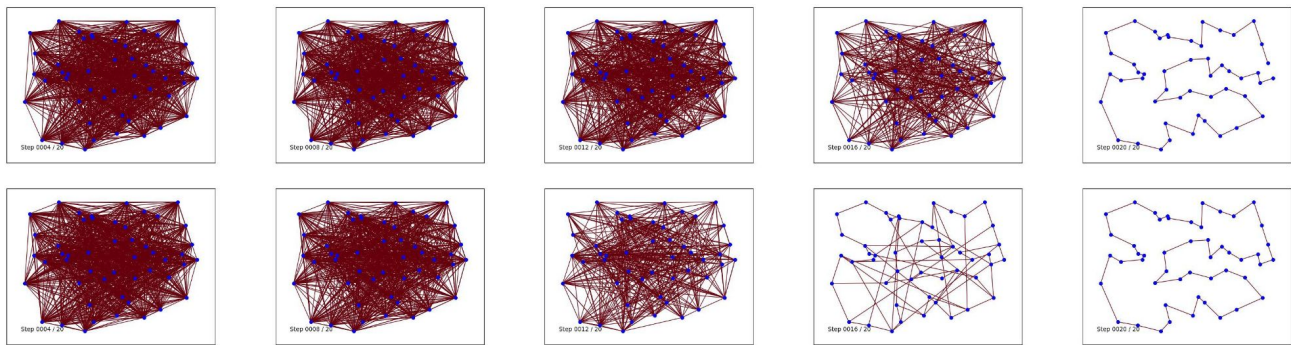


Figure 10: Qualitative illustration of how diffusion schedules affect the generation quality of **discrete** diffusion models. The results are reported without any post-processing. **Discrete** DIFUSCO with `linear` schedule (first row) and `cosine` schedule (second row) with 20 diffusion steps are shown.

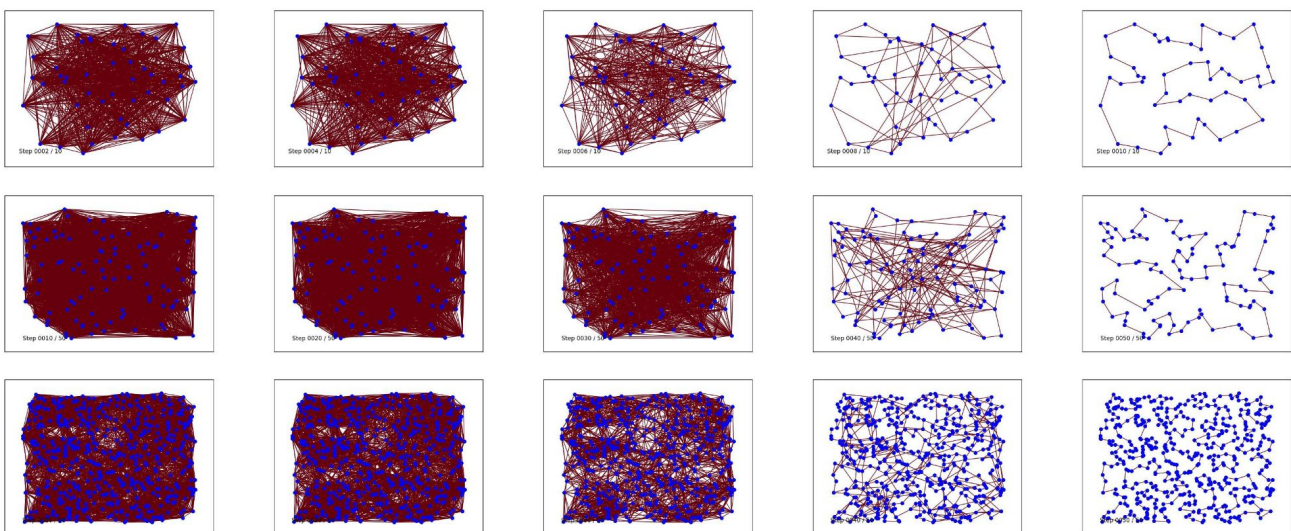


Figure 11: Qualitative illustration of discrete DIFUSCO on TSP-50, TSP-100 and TSP-500 with 50 diffusion steps and `cosine` schedule.

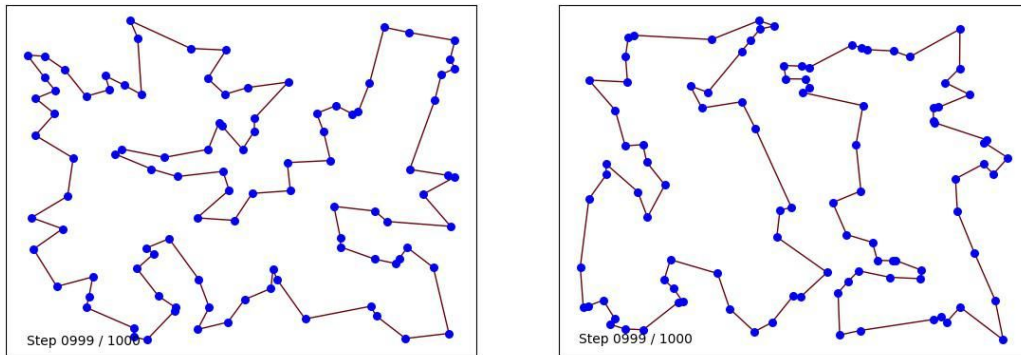


Figure 12: Success (left) and failure (right) examples on TSP-100, where the latter fails to form a single tour that visits each node exactly once. The results are reported without any post-processing.